Supramolecular Hybrid Hydrogel Synthesis and Characterization for Burn Wound Dressing Applications

Thesis submitted by
Zosia Stafford

In Partial Fulfillment of the Requirements for the
Degree of
Master of Science in Materials Science and Engineering

TUFTS UNIVERSITY
Somerville, Massachusetts

February 2024
Advisor: Ayse Asatekin

ABSTRACT

Burn wounds affect over 400,000 people in the US annually and are the sixth most common cause of preventable injury-related death in the US. Despite the severity and prevalence, there is yet to be an ideal wound dressing for burn treatments. This thesis proposes the use of a supramolecular hybrid hydrogel for burn wound dressings and other biomedical applications. These hydrogels are prepared by mixing a polymer containing quaternary amine groups with cucurbit[7]uril molecules that cross-link using supramolecular interactions, with clay nanosheets included to enhance mechanical properties. This thesis aims to better understand the link between hydrogel composition with resultant mechanical properties and dissolution behavior, investigating the effect of polymer chemistry as well as concentrations of each component and mixing order. These hybrid hydrogels demonstrate extensive tunability and improved manufacturing methods, giving important insights into the link between supramolecular interactions and material properties.

ACKNOWLEDGMENTS

I would like to thank my advisor, Ayse Asatekin, my peers in the Asatekin and Panzer labs, especially Luca Mazzaferro, and colleagues at Massachusetts General Hospital, particularly A. Aslıhan Gökultan, for their continuous support and motivation throughout this process. I would also like to thank the Chemical Engineering department for the lab space and facilities, the Electrical Engineering department for the advising and academic support, the Mechanical Engineering department for the endless encouragement and rich community, and the Philosophy department for their bemused but supportive spirit. My Masters' degree would not have been possible without the tireless faculty and professors who offered their time and energy to assist me along the way - you all inspired me to stay curious and persistent in my work. A special thank you to those who have been supporting me throughout my entire college career - Brandon Stafford, Kristen Wendell, Briana Bouchard, Mike Zimmerman, George Smith, and Avner Baz in particular - as well as many more who have played a crucial role in my academic success. I am endlessly appreciative of your kindness and interest in my development as a student and member of the community.

TABLE OF CONTENTS

LIST OF ILLUSTRATIONS

LIST OF TABLES

NOMENCLATURE

AH. Amantadine hydrochloride.

AIBN. Azobis(isobutyronitrile).

CB[7]. Cucurbit[7]uril hydrate.

CCH. Chemically cross-linked hydrogel.

CNS. Clay nano-sheets.

DIW. De-ionized water.

DMSO. Dimethyl sulfoxide.

Hydrogel. 3D polymer network able to absorb and retain large amounts of water.

MEHQ. 4-methoxypheno.

MMA. Methyl methacrylate.

PAM. Poly(acrylamide-*random*-(3-methacryloylamino) propyl trimethylammonium chloride) (Am-*r*-MATMAC) .

PBS. Phosphate buffered saline.

PCH. Physically cross-linked hydrogel.

PEI. Polyethylenimine.

PMM+. Poly(methyl methacrylate-*random*-3-(methacryloylamino) propyl trimethyl-ammonium chloride) (P-MMA-*r*-MATMAC).

PMPC. Poly(2-methacryloyloxyethyl phosphorylcholine).

SHH. Supramolecular hybrid hydrogel.

SPA. Sodium polyacrylate.

TEMED. Tetramethyl ethylenediamine.

Zwitterion. Polymer that contains both positively and negatively charged components.

Chapter 1

INTRODUCTION

This thesis aims to investigate the link between the formulation and manufacturing method of a new family of supramolecular hybrid hydrogels (SHHs) for use in burn wound dressings with their mechanical properties. There is an immediate need for these kinds of dressings, as traditional dressings adhere to the skin and impede uninterrupted healing. Patients with burns and their medical practitioners are in need of a dressing that can increase efficiencies in the hospital by reducing dressing change times, pain killer usage, and duration of patient hospital stay. This thesis proposes a hydrogel that can be easily synthesized, applied to the skin to promote healing and allow for monitoring, and then be dissolved on-demand.

Our group has recently developed novel SHHs for use in this field (Gokaltun, 2023). The initial formulations in this study showed promising performance in terms of mechanical properties and dissolubility. However, this study was an initial proof of concept. A deeper study of the interactions between different components forming these SHHs is needed to better understand how we can tune and control the properties of this new material family, and to further optimize its use for various applications. Furthermore, only one polymer formulation was tested previously, while many other potential polymeric components are conceptually possible. Motivated by these unanswered questions, this thesis aims to expand the range of hydrogel compositions to better discern how each component affects the overall material properties of the hydrogel, as well as their dissolubility.

This thesis begins with information regarding current needs in burn treatments, plus general background on hydrogels, supramolecular interactions, and previous work from our lab. We then discuss methodology, including materials used and charac-

terization techniques, before delving into the results of extensive hydrogel testing. These results include changes to manufacturing methods, effects of changes to component concentration on mechanical properties, mixing order, ease of dissolubility, and proposed alternative polymers. Finally, this thesis considers possible directions for future studies.

Chapter 2

BACKGROUND

2.1 Burn treatments

Emergency departments see over 400,000 cases of burn-related injuries annually, with over 3,000 of these resulting in death (Evans, 2022). Since 2005, burns have been the sixth most common cause of preventable injury-related death in the US, for all age groups (Council, 2023). This risk is increased for age groups under 9 and over 55. Globally, burns are the fourth most common injury, and over 11 million cases require medical attention annually (Peck, 2011). These numbers have decreased over the years but disproportionately affect low- and middle- income countries (LMIC), with 90% of burn deaths occurring in LMIC. And even in high-income countries like the US, lower socioeconomic status is the greatest risk factor in burn susceptibility (Peck, 2011).

The economic cost of burn care is high, with most patients requiring specialized treatment at burn units and long periods of rehabilitation (Yu, 2020). Factoring in all healthcare related costs, the total cost per patient with burns in high-income countries is an average of $88,000. This is drastically more expensive than other special treatment units like trauma or acute surgery, which average $17,245 and $26,468 respectively across high-income countries (Hop, 2014). In the US specifically, it costs hospitals an average of $94,000 per surviving patient and $309,000 per non-surviving patient (Mosier, 2016). Additionally, some studies suggest that direct healthcare costs account for only 10% of total societal costs, like indirect costs due to productivity loss (Hop, 2014). The total burn surface area (TBSA) is a reliable predictor of cost; there is an average healthcare cost of $4,000 per 1% TBSA, though this metric fails at >80% TBSA due to high mortality rates (Hop, 2014).

Additionally, the most expensive burn care component is hospital stay - by reducing time in the hospital, associated healthcare costs can be significantly reduced. In the US, the average hospital stay is 9.7 days for surviving patients and 15.7 days for non-surviving patients (Mosier, 2016).

Burns can be incredibly painful injuries, with severe pain reported at every stage of the healing process (Duchin, 2021). Pain management is crucial for recovery. It strengthens confidence in the medical team, ensures that burn hypermetabolism, which is linked to increased pain, is kept low, and reduces patient reliance on opioids (Latarjet, 1995). There is extreme variability of patient pain ratings which can be hard to predict, but the most severe pain is consistently reported during therapeutic procedures like dressing changes and wound debridement. These are carried out frequently and over long periods of time, leading many to describe the procedures as the most painful experience of their lives (Choinière, 1989). Opioids remain the principal treatment for pain management, but in recent years a number of opioid-sparing techniques have risen in pertinence, such as multimodal analgesia, or even nonpharmological approaches like virtual reality (James, 2017).

Currently, there is no "gold standard" for burn wound dressings. The most common dressing materials are silver-based dressings, paraffin-impregnated gauze, or dry materials (usually simply gauze) (Opriessnig, 2023). However, these are imperfect solutions that typically interfere with the healing process. Silver-based dressings, such as those with a silver sulphadiazine cream, take advantage of the antimicrobial properties of silver. However, there are possible side effects like silver allergies, staining of the wound, and hyperosmolality (Selig, 2012). Silver sulphadiazine has also been linked to a toxic effect on regenerating keratinocytes, which can delay healing (Wasiak, 2013). Wound dressings with gauze have the tendency to adhere to the skin, which necessitates debridement at every dressing change and traumatizes new epithelialized skin. This is an extremely painful process which can lead to an

increased use of opioids and delayed healing as the wound is disturbed (Latarjet, 1995). The doctors also must change this dressing fairly frequently to inspect the wound, as it is opaque and doesn't allow for external monitoring (Siavash, 2023). Most doctors suggest dressing changes either twice weekly or on alternate days, which means any trauma to the wound is frequent and significantly delays healing (Selig, 2012). As the wound is disturbed and uncovered, risks of infection also increase. Infection is the leading cause of death in burn patients; in a study over the last decade, 54% of burn deaths were due to sepsis from infection (Williams, 2009). Even if infection is avoided, the frequent dressing changes and continuous damage to healing skin means patients must stay in hospital care for longer, which leads to higher patient costs.

In a study of 200 medical experts from 50 countries, the characteristics considered "extremely important" for an ideal burn wound dressing were lack of adhesion, pain-free dressing change, and fewer dressing changes (Opriessnig, 2023). There were no significant regional differences amongst the "extremely important" characteristics, indicating that global experts are in agreement about priorities for an ideal dressing. In a separate study of 120 experts from 40 countries, 50% said the most important burn wound dressing characteristic is a "non-adherent, non-traumatic wound interface" (Selig, 2012). Globally, medical experts agree that wound adhesion of dressing is a critical issue in burn care - it increases patient pain and slows healing, which contributes to longer hospital stays and subsequent high costs for hospitals. There is yet to be a satisfactory solution, and the patients would greatly benefit from such a dressing. Other priorities for a burn wound dressing are antimicrobial activity, self-adhesion, absorbency, non-bulkiness, and availability in a range of different sizes (Selig, 2012).

Hydrogels have been proposed as a more ideal burn wound dressing, as they address many of the shortcomings of current dressings (Celik, 2023). They are able to

incorporate antimicrobial properties, keep the wound moist, can absorb wound exudates, and most importantly, offer new methods to eliminate surface adhesion (Xu, 2017). Several other hydrogel solutions are used or in development, but they generally have poor mechanical properties, are hard to dissolve (or take a long time, or become unstable), are complicated to synthesize, or are untested *in vivo* or *in vitro* and are not biocompatible (Gokaltun, 2023). The majority of hydrogels in production are chemically cross-linked, which typically still adhere to the wound to some degree, and those that are dissolvable have long dissolution times (>30 min) (Konieczynska, 2016).

This thesis focuses on the mechanical and physical behavior of a novel hydrogel dressing family that is fully dissolvable within minutes, has strong mechanical properties, is simple to synthesize and apply, and can incorporate antimicrobial properties. It is also transparent, which allows for external monitoring of the wound. A burn dressing with these properties will be significantly beneficial to burn centers and the healthcare industry in general - patient pain can be reduced, and healing accelerated, which will minimize dressing change time and hospital stay length, which in turn decreases the economic burdens of burn care.

2.2 Hydrogels

Hydrogels are a type of three-dimensional polymer network able to imbibe a large quantity of water. They can be synthesized by natural or artificial means and have a wide range of applications. Due to their high-water content, they are typically flexible and highly tunable. Hydrogels have received increased attention in the last decades, and have numerous applications in biomedical and engineering fields, such as tissue-engineering scaffolds, contact lenses, antifouling coatings, wound dressings, soft robotics, biosensors, drug delivery, physiological membranes (Wang, 2020).

There are many kinds of hydrogels, depending on their polymer components, configuration, bonding, or appearance. Hydrogels may be homopolymeric with a single species of monomer, copolymeric with multiple monomers, or multipolymer interpenetrating if it has two independently cross-linked polymer networks. Hydrogels may also be amorphous, semi-crystalline, or crystalline. Finally, hydrogels can be further divided into two classes depending on the method of cross-linking. Chemically cross-linked hydrogels (CCHs) form permanent cross-linking junctions, while physically cross-linked hydrogels (PCHs) have transient junctions formed from either physical entanglements of polymer chains or noncovalent cross-links from ionic interactions, hydrogen bonding, hydrophobic interactions, or other electrostatic interactions (Ahmed, 2015).

Within PCHs, supramolecular hydrogels (SHs) are a more specific class of hydrogel that are likewise composed of non-covalent cross-links, but containing macromolecules that self-assemble into a hydrogel network (Omar, 2022). Because of these non-covalent bonds, they are easier to dissolve but also are typically mechanically weaker. Supramolecular hybrid hydrogels (SHHs) refer to SHs that are reinforced by integrating inorganic materials to become "hybrid." These inorganic materials, such as clay, can able to provide further structure to the hydrogel and improve mechanical properties (Harada, 2015).

2.3 Desired Mechanical Properties of Hydrogel Dressings

There is no set requirement for SHH stiffness for use in wound dressings. On the lower end, the gel must be stable and stay intact while moving. It cannot be so weak that it falls or drips off and must more-or-less hold its shape. On the other hand, it must be flexible enough to move with the skin without breaking, and not so rigid that it interferes with movement.

When testing, we used the storage and loss moduli to describe the stiffness of the

material. The storage modulus describes how a viscoelastic material stores energy elastically when deforming, and the loss modulus describes its viscous reaction and how the material loses energy through internal friction when flowing. A higher loss modulus indicates more liquid behavior, while a high storage modulus means it behaves more like a typical solid. When a material has no viscous component, the elastic modulus is used instead of storage and loss. The storage and loss moduli specifically describe the material's stiffness; comparing between this particular subset of hydrogels, higher stiffness can be an indicator of higher strength, but they are not synonymous.

The storage modulus for human skin is highly variable. Skin is anisotropic and viscoelastic, making it a difficult material to characterize. Additionally, the properties of the skin depend heavily on its location on the body and the age of the person. Older people have shorter collagen and elastic fibers, which makes their skin significantly weaker (Silver, 2002). Skin is also difficult to characterize because of its complex composition. The dermis and epidermis alone have different properties than the whole organism - underlying tissue and muscle combine with the skin to create a stronger system. Dermis-only tests give a range of 430 to 6600 Pa, which is relatively weak (Holt, 2008). In contrast, using non-invasive methods to measure still-attached skin, researchers found a storage modulus of 12 to 28 kPa (Kearney, 2015). There have also been some studies that analyze skin as a linear elastic semi-infinite material by including the effects of underlying layers. These studies have an even larger range of results, one such study looking at indentation on the tibia finding elastic moduli from 10 to 90 kPa using quasistatic measurement speeds (Kalra, 2016).

This large range of values means there is little guidance on the best benchmark for hydrogel stiffness. Rather than design a hydrogel of a specific storage modulus, the goal of this thesis was to better understand the internal interactions of SHHs and

how composition affects the resultant modulus. For a functional wound dressing, the hydrogel should not be too far below the modulus of skin dermis, so ideally above 400 Pa, and not far above the modulus of the whole structure, so not above 90 kPa. Using the chosen components, the synthesized SHHs in this thesis are all within this range, meaning they would be practical for use as a wound dressing.

2.4 Supramolecular Interactions

Supramolecular interactions are types of non-covalent interactions between individual molecules, rather than within a molecule. These interactions, as shown in Figure 2.1, include hydrophobic interactions, hydrogen bonding, ionic interactions (also called electrostatic interactions), metal-ligand interactions, π-π bonding, van der Waals interactions, and host-guest interactions. These interactions are typically weaker than any covalent bond and are reversible, which can allow systems with supramolecular interactions to be more stimuli-responsive and have a more complex architecture. The SHHs in this thesis rely on a combination of electrostatic interactions and hydrogen bonding. One major mechanism is that of a host-guest interaction, in which two molecules form a 1:1 binary complex and interact with the cavity of a larger molecule, as seen in Figure 2.2. This study focuses on cucurbit[7]uril (CB[7]), a macrocycle containing 7 glycoluril units bound together by 14 methylene bridges (Barrow, 2015). These macrocyles can be formed with 5, 6, 7, 8, or 10 glycoluril units, thus named CB[5], CB[6], *etc*. The diameter of the ringed structure increases each time - CB[7] has a portal diameter of 5.4 Å, a cavity diameter of 8.8 Å, an outer diameter of 17.5 Å, and a height of 9.1 Å(Barrow, 2015). The portal of this molecule is highly electronegative and encourages smaller molecules to interact.

As a result, insertion complexes where the component is fully housed in the CB[7] can form. This is often termed a “host-guest” interaction. In contrast, an exclusion

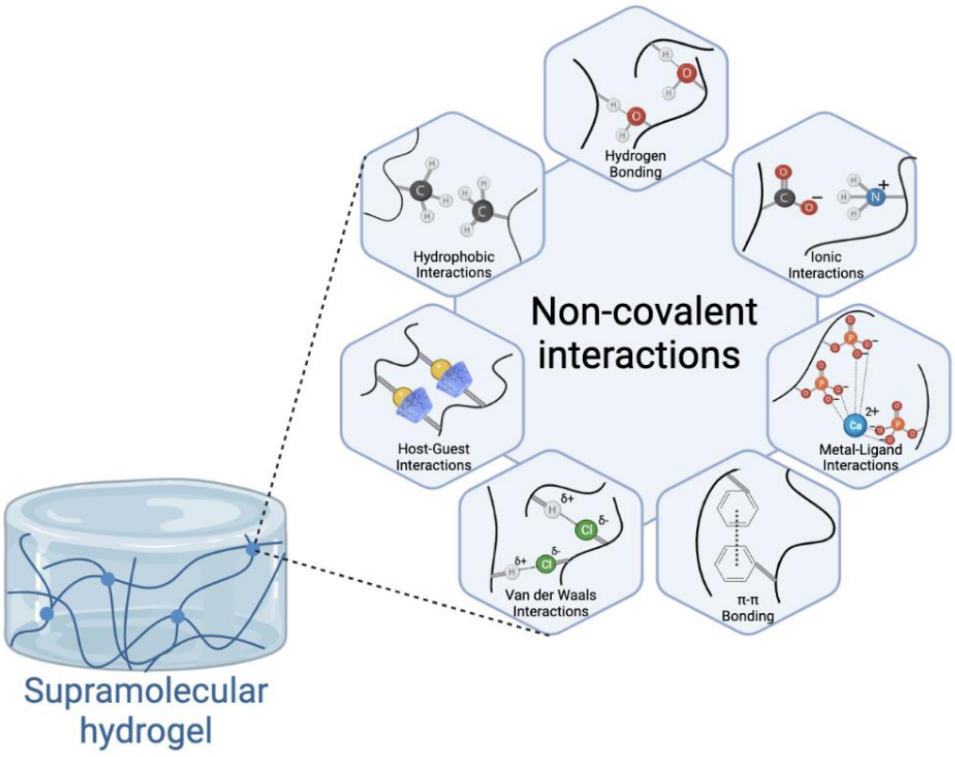

Figure 2.1: Diagram of possible non-covalent interactions within a supramolecular hydrogel (Omar, 2022).

complex will have only a small portion of the guest molecule inside the ring of CB[7]. Affinity is determined by a few factors like binding affinity or the physical compatibility of molecules, where the inner cavity of the host is large enough for the guest (Barrow, 2015). Host-guest interactions are often stronger than many other supramolecular interactions. These interactions have been used to make hydrogels for various applications, where competitive interactions can be used to dissolve these gels on demand. It allows for more precise tunability and fast responses to external stimuli. However, these hydrogels are often mechanically weak and can be toxic for human use, plus the synthesis of host-containing polymers can be very complex (Omar, 2022). We seek to develop a simpler and more sustainable synthesis process, resulting in hydrogels that are both mechanically robust and biocompatible.

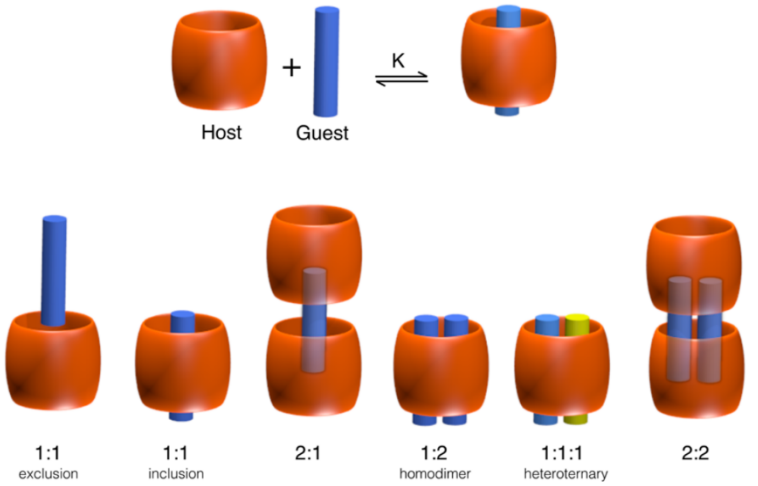

Figure 2.2: Types of host-guest interactions (Barrow, 2015).

2.5 Cucurbituril-based SHHs for Burn Wound Dressings

Previous work on this research describes the formation of an SHH that is biocompatible, self-healable, and on-demand dissoluble for use in burn wound dressings. These SHHs are prepared by a simple, fast, and scalable method, using host-guest chemistry with cucurbit[7]uril (CB[7]) and the cationic copolymer poly(acrylamide-*random*-(3-methacryloylamino) propyl trimethylammonium chloride) (Am-*r*-MATMAC, called PAM), as well as electrostatic interactions with clay nanosheets (CNS) coated with an anionic polymer sodium polyacrylate (SPA) to achieve enhanced mechanical properties and fast on-demand dissolution. The main mechanism for this formation is shown below in Figure 2.3, were PAM is the guest and CB[7] the host, which along with SPA and CNS form the SHH. With a more competitive guest, the host-guest interaction between CB[7] and PAM is broken and the hydrogel dissolves. The SHHs show high mechanical stiffness of up to 50 kPA, self-heal rapidly in about 1 min, and dissolve quickly (4–6 min) using an amantadine hydrochloride (AH) solution that breaks the supramolecular interactions in the SHHs. This study also shows that neither the SHHs nor the AH solution have any adverse effects on human dermal fibroblasts or epidermal keratinocytes *in vitro*.

The SHHs also do not elicit any significant cytokine response *in vitro*. Furthermore, *in vivo* murine experiments show no immune or inflammatory cell infiltration in the subcutaneous tissue and no change in circulatory cytokines compared to sham controls (Gokaltun, 2023).

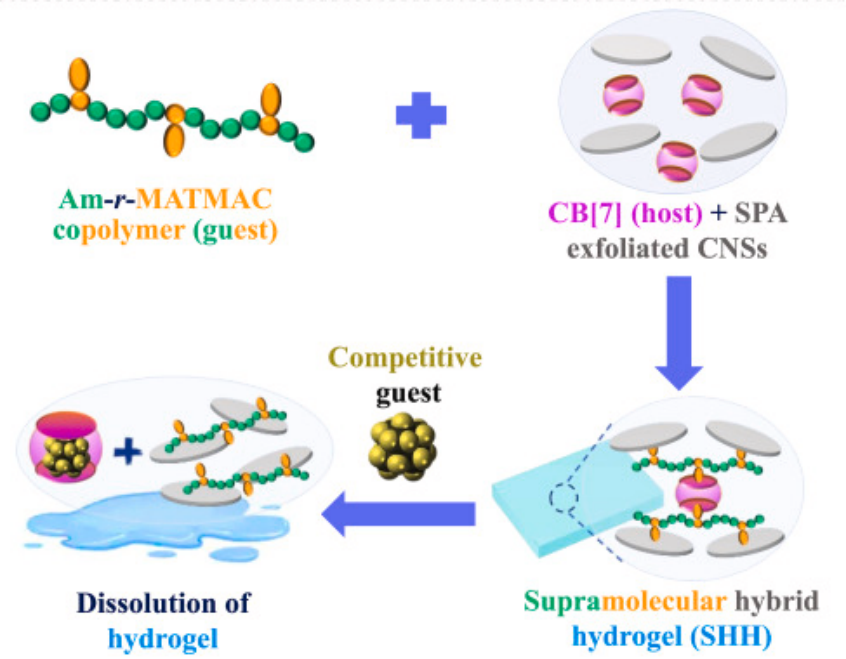

Figure 2.3: Mechanism of SHH formation using AM-*r*-MATMAC as a guest and CB[7] as a host, allowing for easy formation and dissolution (Gokaltun, 2023).

This study offers an excellent proof of concept for this SHH material family, demonstrating its potential for use in burn wound dressings. Based on this work, a deeper study of the supramolecular interactions at work within these SHHs will be useful to better understand the connection between individual components and mechanical properties. We will also explore different polymeric structures beyond just PAM. This will further refine our understanding and allow us to tune and control the properties of this new material family more precisely to optimize it for various applications.

2.6 Thesis Objective and Rationale

We aim to characterize how changing various components of the SHH formulation affects mechanical properties and dissolution. We synthesized and tested hydrogels formed from two polymers and a wide range of compositional formulas, investigating the effect of polymer chemistry, component composition, and mixing order. The interactions between each polymer and cucurbituril molecules within the hybrid hydrogel structure were analyzed to better understand how each composition affects mechanical and chemical properties. This material investigation consists of analyzing rheological properties like storage modulus and performing dissolution testing.

Chapter 3

METHODOLOGY

3.1 Materials

Acrylamide (Am), [3-(Methacryloylamino) propyl] trimethylammonium chloride solution, 50 wt% in H_2O (MATMAC), cucurbit[7]uril hydrate (CB[7]), sodium polyacrylate (SPA), amantadine hydrochloride (AH), and N, N, N', N'-Tetramethyl ethylenediamine (TEMED) were all purchased from Sigma Aldrich (St. Louis, MO). Laponite XLG-XR clay nanosheets (CNS) were acquired from Acme-Hardesty Co. (Blue Pell, PA). Acetonitrile (ACN) was obtained from Thermo Fisher Scientific (Waltham, MA). Azobis(isobutyronitrile) (AIBN), 4-methoxyphenol (MEHQ), 2-methacryloy-loxyethyl phosphorylcholine (MPC), polyethylenimine (PEI) (average Mw ~25,000 by LS, average Mn ~10,000 by GPC, branched), phosphate buffered saline (PBS) packets were purchased from Sigma-Aldrich (St. Louis, MO). Deuterium oxide (D2O) was obtained from Cambridge Isotope Laboratory. Methyl methacrylate (MMA), and dimethyl sulfoxide (DMSO) were obtained from Fisher Scientific (Waltham, MA). All chemicals and solvents were of reagent grade and used as received.

3.2 Synthesis of Polymers

The polymer poly(2-methacryloyloxyethyl phosphorylcholine) (PMPC) was synthesized following a free radical polymerization. First, 5 g MPC was dissolved in 40 mL of dimethyl sulfoxide in a 100 mL round bottom flask at room temperature. Then 0.005 g of the initiator AIBN was added after dissolution. The reaction mixture was purged with nitrogen for 30 min to purge any dissolved oxygen. The flask was then placed in an oil bath set to 60 °C, while stirring at 300 rpm for 20 hours. The

flask was removed from the oil bath and unsealed, and 0.5 g of MEHQ was added to terminate the reaction. The reaction mixture was then precipitated in acetone and purified by stirring three fresh portions of 8% methanol and 92% acetone by volume for at least 3 hours to eliminate any remaining unreacted monomer. The attained solid polymer was dried for two days under a fume hood and two more days in a vacuum oven at 50 °C. The product yield was 45% and calculated from the ratio of the mass of the product polymer to the mass of the monomer used. The chemical composition of the polymer was verified by ^{1}H-NMR (Bruker Avance III 500 MHz spectrometer, using D_2O) (Asatekin, 2023).

The random copolymer poly(acrylamide-*random*-(3-methacryloylamino) propyl trimethylammonium chloride) (Am-*r*-MATMAC, called PAM) was synthesized following a free radical polymerization seen in Figure 3.1 below. Briefly, 6 mL MATMAC and 7 g Am were dissolved in 100 mL distilled water in a 250 mL round bottom flask at room temperature. 0.1 g of the initiator AMPS was added after dissolution. The reaction mixture was then purged with nitrogen for 15 min. Then, 0.067 mL TEMED in 0.5 mL water was added into the mixture dropwise with a syringe. After another 15 min of nitrogen purge, the reaction was conducted by stirring at 250 rpm for an hour at room temperature (25 °C). Then, the reaction mixture was poured into a 1:1 mixture of ACN and reagent alcohol to precipitate out the copolymer, followed by three successive washes to eliminate any remaining unreacted monomer. The final solid polymer was dried for two days under a fume hood and two more days in a vacuum oven at 50 °C. The product yield was 75% and calculated from the ratio of the mass of the product copolymer to the mass of the monomers used. The product was determined to contain 46% MATMAC monomer using NMR spectroscopy in DMSO-d_6 (Gokaltun, 2023). We also considered the polymer PMM+, or poly (methyl methacrylate-*random*-3-(methacryloylamino) propyl trimethylammonium chloride) (MMA-r-MATMAC, called PMM+). It was synthesized following a free

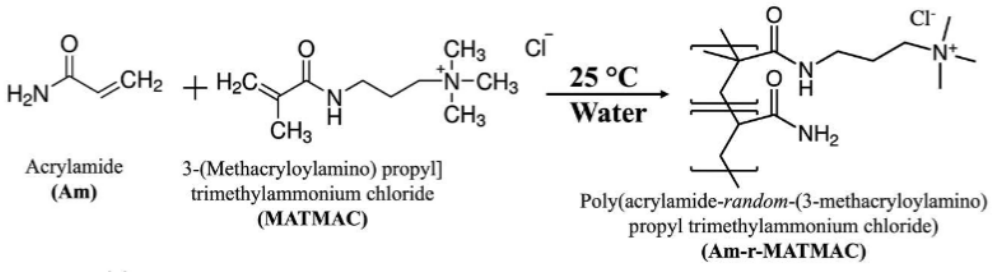

Figure 3.1: Synthesis of Am-*r*-MATMAC using free radical polymerization (Asatekin, 2023).

radical polymerization. Briefly, 5.5 mL MATMAC (50% water) and 2.25 g MMA were dissolved in 22 mL DMSO in a round bottom flask at room temperature. 0.005 g of the initiator (AIBN) was added after dissolution. The reaction mixture was purged with nitrogen for 30 min to purge any dissolved oxygen. The flask was then placed in an oil bath set to 60 °C, while stirring at 300 rpm for 20 hours. The flask was removed from the oil bath and unsealed, and 0.5 g of MEHQ was added to terminate the reaction. The reaction mixture was then precipitated in acetone and purified by stirring three fresh portions of 10% methanol and 90% acetone by volume for at least 3 hours to eliminate any remaining unreacted monomer. The attained solid polymer was dried for two days under a fume hood and two more days in a vacuum oven at 50 °C. The product yield was 60% and calculated from the ratio of the mass of the product polymer to the mass of the monomer used.

3.3 Synthesis of Hydrogels

Each component was initially made into a bulk solution; this included a 4-6 wt% solution of CNS, 2 wt% solution of CB[7], and a 2.5-5 wt% solution of polymer. Polymers tested included PMPC, PAM, PEI, and PMM+. Then, depending on the composition of the SHH, appropriate amounts were micropipetted from these bulk solutions. Several controls were synthesized - their synthesis followed the same general procedure.

Each SHH that was tested was synthesized in a 10 ml glass vial, and 2 ml of total solution was made. First a CNS solution was added. Then deionized water was added to ensure the final hydrogel was 2 ml. This was vortexed for 30 sec until mixed. Then, the CB[7] solution was added and immediately vortexed for 30 sec. After 10 min, the polymer solution was added and immediately vortexed for another 30 sec. After 15 min, the sample could be tested on the rheometer. More detailed information regarding composition of hydrogels can be found in appendices B-E.

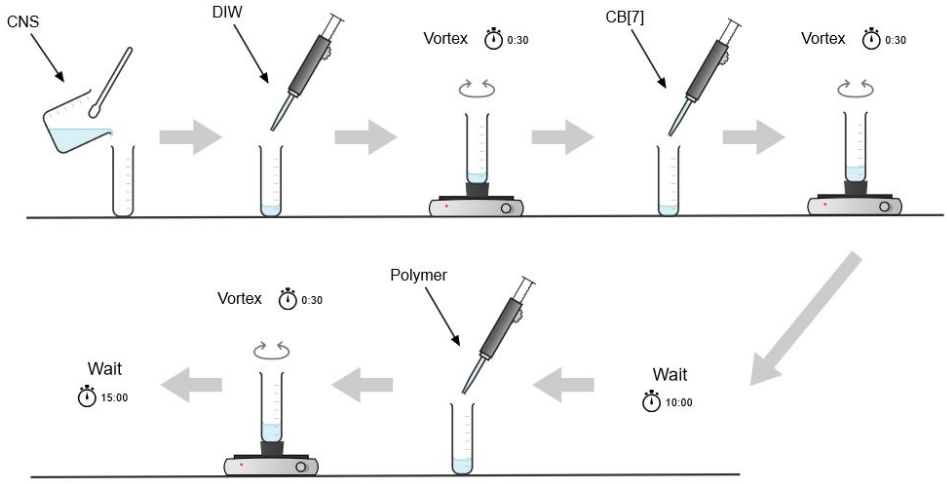

Figure 3.2: MATMAC monomer chemical structure.

3.4 Hydrogel Characterization

Rheological testing was the main characterization technique used in this thesis, as we wished to investigate the mechanical properties of these hydrogels. Initial testing was performed using Dynamic Mechanical Analysis (TA Instruments, RSA III, New Castle, DE), but the hydrogels were soft enough that rheometry was determined to be the preferred characterization method.

Rheometer Testing

The rheological properties of the SHHs were measured at 25 °C using a rheometer (TA Instruments, Discovery HR 30 Rheometer, New Castle, DE) fitted with parallel

plates (diameter 20 mm). The samples (about 1mL of hydrogel) were placed between the para-plate and the platform, and the plate was lowered to a gap of 1 mm. Any excess hydrogel outside of the 20 mm plate was carefully removed before testing. Dynamic frequency sweep tests (0.1–80 rad/s) at a fixed strain of 0.5% were measured to determine the storage modulus (G') and loss modulus (G") of hydrogels. Two to three batches of SHHs were tested for rheological tests, and SHHs were never tested more than 2 hours after synthesis. Selected graphs of raw data from the rheometer can be seen in Appendix B.

Dissolution Testing

The hydrogels were tested on their ability to dissolve on demand. First, a PBS solution was prepared from powder, with a pH of 7.4 Approximately 0.1 g of each hydrogel was placed onto a Petri dish. The hydrogels were initially exposed to 0.2 mL of the PBS 1x solution for 2 min and gently tapped with a pipette bulb to simulate a wound cleaning procedure, with little pressure applied. After these initial 2 min, the hydrogels were exposed to an additional 0.2 mL of the PBS 1x solution and again gently tapped. After 4 min from the initial exposure final pictures were taken. This process was also performed with 40 mM amantadine hydrochloride (AH) in DI water as the dissolution agent instead of PBS.

^{1}H NMR Spectroscopy

NMR spectroscopy was used to verify the chemical composition of each polymer and their interactions with CB[7]. Testing was performed by ^{1}H NMR (Bruker Avance III 500 MHz spectrometer, DMSO-d6). The binding interaction between the host (CB[7]) and the guest (Am-*r*-MATMAC and PMPC) was also confirmed by ^{1}H NMR in a neutral D_2O solution using different CB[7] and polymer ratios.

Chapter 4

RESULTS AND DISCUSSION

4.1 Material Selection

A major goal of this work was to study the effects of a different polymer structure on mechanical behavior and hydrogel dissolution. To that end, we selected two main polymers to test in more detail. PAM had been included in a previous study on CB[7]-based SHHs, and PMPC was a new, zwitterionic polymer that had yet to be studied in relation to these hydrogels (Gokaltun, 2023).

The first polymer considered was Poly(acrylamide-*random*-(3-methacryloylamino) propyl trimethylammonium chloride, called P(Am-*r*-MATMAC) or PAM in this text. Its chemical structure can be seen in Figures 4.1 and 4.2. It is a water-soluble copolymer combining hydrophilic acrylamide (Am) segments with positively charged quaternary amine MATMAC segments. The MATMAC sections interacts strongly with CB[7], as the cationic copolymer interacts with the highly electronegative portals of CB[7] molecules. The acrylamide groups are hydrophilic and biocompatible, which improves the hydrations and fluid uptake of the hydrogel. It was synthesized by free radical polymerization, as described in Section 3.2 (Gokaltun, 2023).

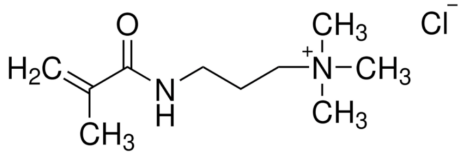

Figure 4.1: MATMAC monomer chemical structure.

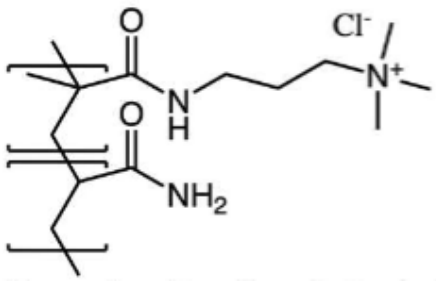

Figure 4.2: Am-*r*-MATMAC co-polymer chemical structure.

The second polymer used for synthesizing SHHs was PMPC, poly(2-methacryloyloxyethyl phosphorylcholine), as seen in Figures 4.3 and 4.4. This polymer is zwitterionic, meaning that it contains both positively and negatively charged components but is overall neutral. The MPC monomer interacts with CB[7] through partial electrostatic interactions, meaning it can be used as the "guest" in the host-guest interaction. As discussed in Section 3.2, PMPC was synthesized by free radical polymerization. As

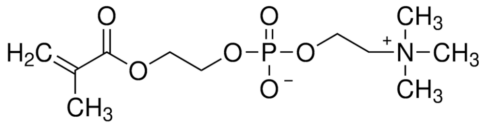

Figure 4.3: MPC monomer chemical structure.

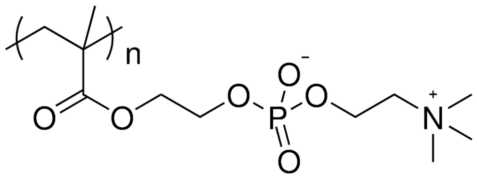

Figure 4.4: PMPC polymer chemical structure.

in the previous study, cucurbit[7]uril, seen in Figure 4.5, was used as a supramolecular cross-linker due to its ability to interact strongly with PAM and PMPC (Gokaltun, 2023). As shown in Figure 4.6, the portals of CB[7] are highly electronegative, with the inside region being fairly hydrophobic as there are no functional groups with

electron pairs accessible from within the cavity. This high electronegativity allows for interactions with the polymers, as they form non-covalent bonds with the portal region of CB[7]. When a more competitive guest molecule is present, CB[7] will preferentially interact with that molecule, allowing for simple dissolution. Clay

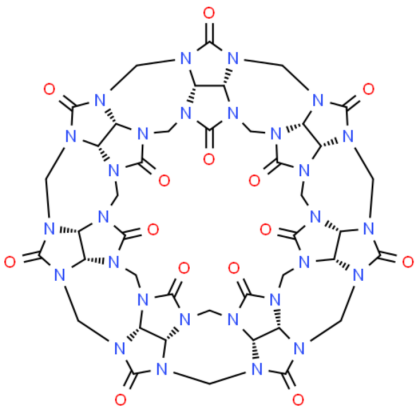

Figure 4.5: Cucurbit[7]uril chemical structure.

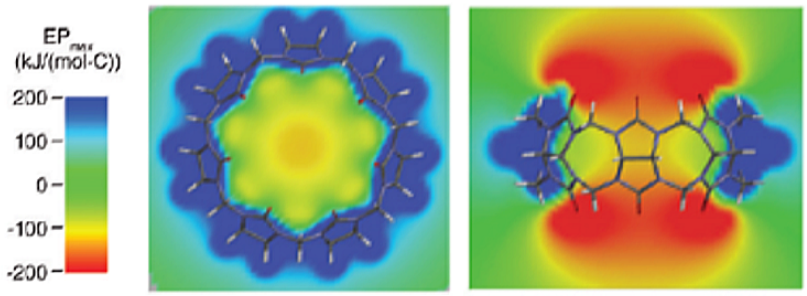

Figure 4.6: Cucurbit[7]uril electrostatic interactions. (Barrow, 2015)

nano-sheets, or CNS, was used to give structure to the hydrogels and enhance the mechanical properties of the SHHs. We used laponite XLG-XR, which is a synthetic smectite clay, consisting of nanocrystal disks. The surface of these disks contains a net negative charge, with positive ions on the sides, as seen in Figure 4.7. When added to water, CNS forms a colloidal dispersion. When other ions or polar molecules are added to this dispersion, the attractive forces become dominant, and

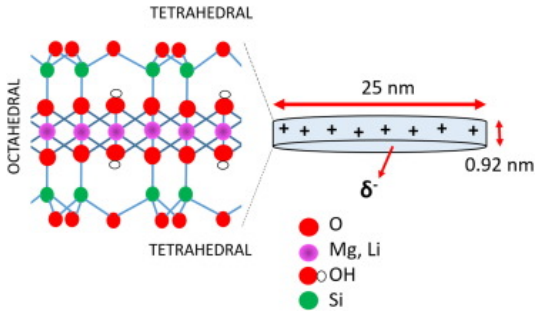

Figure 4.7: Laponite XLG-XR (CNS) chemical structure (Tomas, 2018).

a hydrogel forms (Tomas, 2018). SPA, or sodium polyacrylate, was used initially to stabilize CNS and increase mechanical properties of the hydrogel. The anionic SPA interacts with the cationic edges of CNS, helping it disperse and stabilize (Gokaltun, 2023). It's chemical structure is shown below in Figure 4.8.

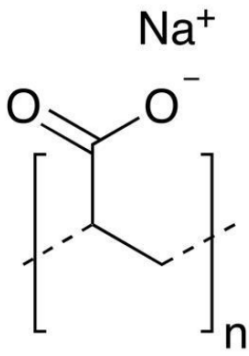

Figure 4.8: SPA chemical structure.

4.2 ^{1}H NMR Spectroscopy

After synthesizing the polymers, ^{1}H NMR spectroscopy was used to confirm their composition, which can be seen in Appendix A, Supporting Info. ^{1}H NMR spectroscopy can also offer insights into how different molecules interact through supramolecular interactions. Here, we used ^{1}H NMR spectroscopy was used to study the interactions between CB[7] and the monomers MATMAC and MPC.

NMR analysis was performed on mixtures of CB[7] and MATMAC monomer to determine the interactions between these groups, as seen in Figure 4.9 below. The

monomer was used because NMR peaks broadened when using the copolymer, as is expected in low diffusivity systems. Peaks associated with MATMAC show significant shift, indicating a close association between MATMAC and CB[7] through partial electrostatic interactions. We can see shifts in the peaks of hydrogens surrounding the cationic charge, which suggests shielding effects caused by steric effects and close proximity to other rigid chemical structures, in this case CB[7] (Gokaltun, 2023).

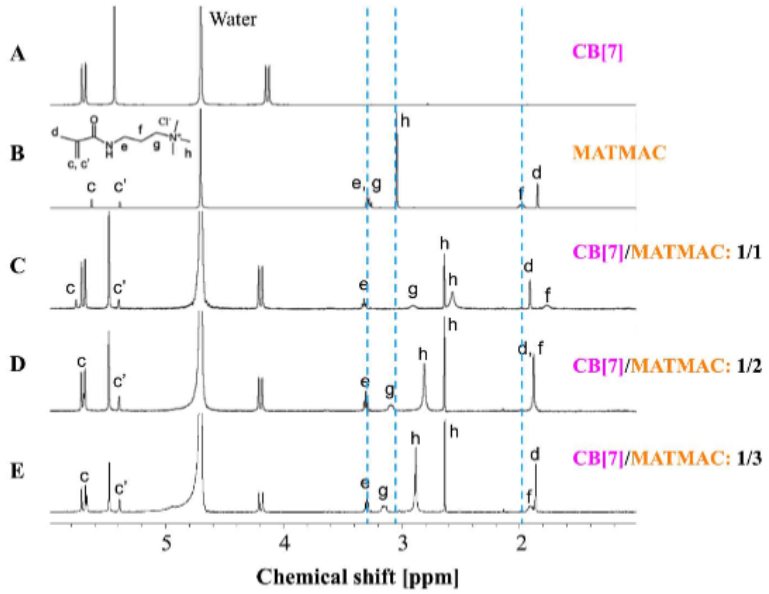

Figure 4.9: NMR of interaction between CB[7] and MATMAC, showing shielding effects (Gokaltun, 2023).

Multiple ratios of MATMAC and CB[7] were tested, and these shifts were seen in all configurations, indicating that at least 2, and potentially more, MATMAC molecules can associate with CB[7], which would lead to cross-linking. Interestingly, chemical shifts in 1:1 CB[7]:MATMAC mixtures were quite different than those observed in 1:2 and 1:3, implying different arrangements for different ratios. Previous literature shows various ways that CB[7] can interact with similar molecules ranging from the insertion of the hydrophobic groups inside the core of the ring (1:1 ratio) and

binding and association of amine groups with CB[7] as well as other CBs (1:2 ratio). Our results imply that MATMAC molecules can potentially form both types of arrangements (Gokaltun, 2023).

NMR analysis was also performed on mixtures of CB[7] and the MPC monomer as a simplified system to determine interactions between these groups, seen in Figure 4.10. We observed that peaks associated with MPC show significant peak shifts, indicating interactions between MPC and CB[7]. Like with the MATMAC monomer, there are shifts in the peaks of hydrogens surrounding the cationic charge, which are most likely caused by steric effects and close proximity to other rigid chemical structures, in this case CB[7] (Asatekin, 2023).

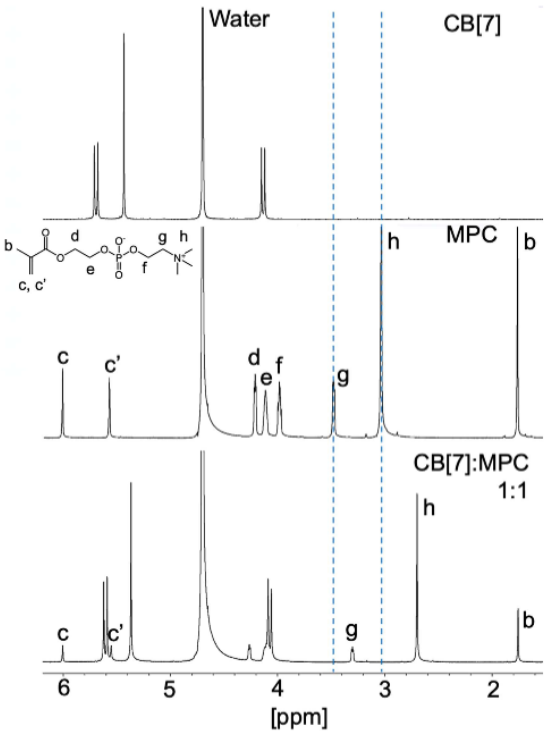

Figure 4.10: NMR of interaction between CB[7] and MPC, showing shielding effects (Asatekin, 2023).

4.3 Hydrogel Formation and General Observations

When synthesizing the SHHs, CNS and water were mixed first, forming a colloidal dispersion. At high concentrations of CNS, this formed a relatively weak hydrogel. Once the polymer and CB[7] were added and vortexed, a strong hydrogel formed within minutes. As seen in Figure 4.11, hydrogels with all components would keep their shape and not flow. Without CB[7], they had lower viscosity, acting more like CNS alone. The SHHs were soft to the touch but would maintain their shape, as can be seen in Figure 4.12. Hydrogels containing PAM were visibly stronger than those containing PMPC, as they were firmer to the touch and more elastic.

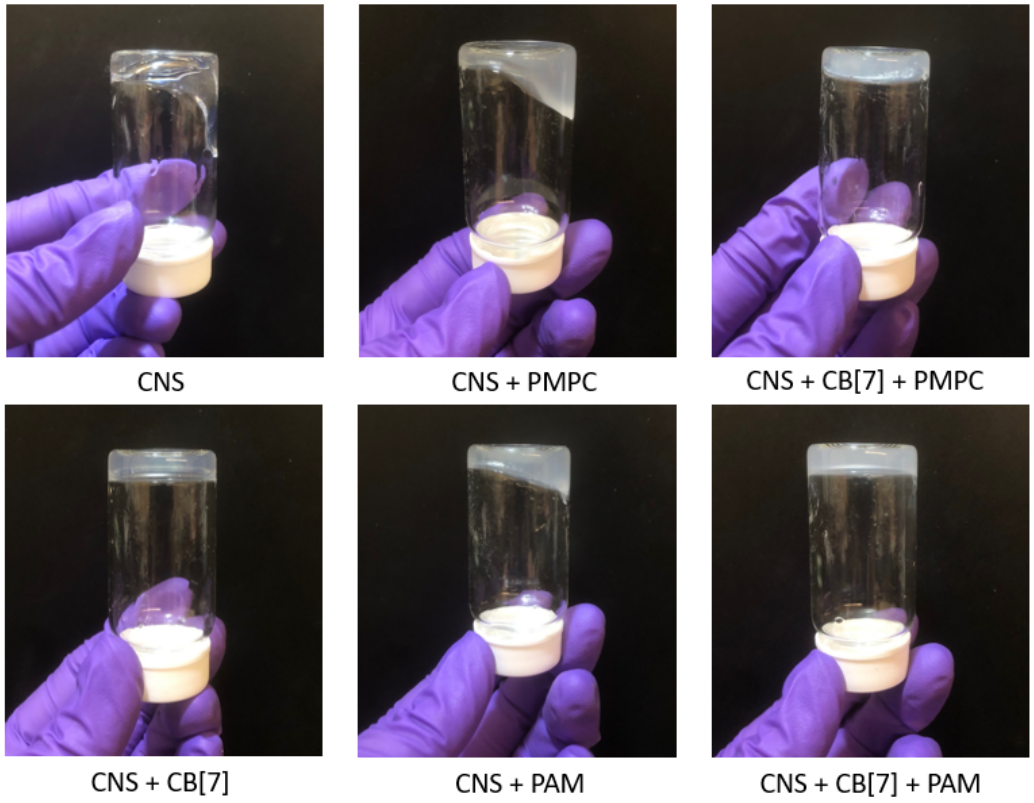

Figure 4.11: General observations of array of hydrogels. From left to right and top to bottom, hydrogels displayed are CNS alone, CNS with PMPC, CNS with CB[7] and PMPC, CNS with CB[7], CNS with PAM, and CNS with CB[7] and PAM. Hydrogels contain 3.2 wt% CNS, 0.26 wt% CB[7] (if included), and 0.25 wt% polymer. Hydrogels without CB[7] had lower viscosity, while those with CB[7] would hold their shape.

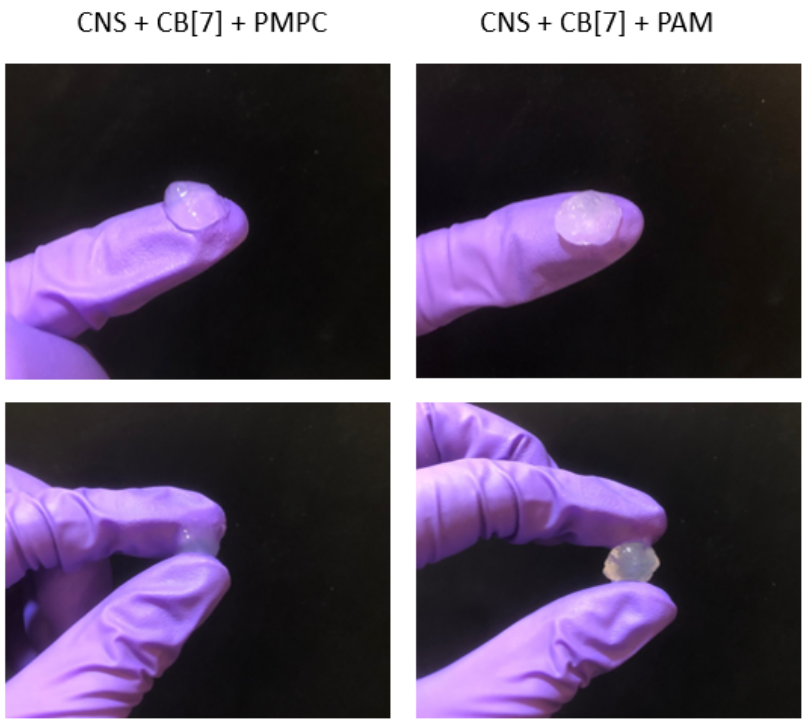

Figure 4.12: General observations of hydrogels. Hydrogels contain 3.2 wt% CNS, 0.26 wt% CB[7], and 0.25 wt% polymer. Hydrogels containing PAM are firmer and more easily shaped than those containing PMPC.

4.4 Effect of SPA on Gel Consistency and Mechanical Properties

Though SPA was a main component in the initial paper on this topic of investigation, we removed SPA early on due to it being a contributing factor in non-homogeneity, its added complexity to the SHH synthesis, and its resistance to dissolution.

When added to water, SPA powder will swell and aggregate to itself, forming many small chunks of material. When added to the hydrogel, these pieces never fully integrate with the CNS and polymer. This created spaces in the SHH where there may be a higher or lower concentration of SPA, which significantly affected the mechanical properties at that spot. This made characterization much more difficult since the SHH was heterogeneous, and its properties were slightly different depending on where it was tested. Also, SPA had the tendency to make water separate out when left sitting. If the hydrogel is not tested immediately, then when

the sample is compressed under the rheometer plate, water will leak out. This leaves a hydrogel with lower water content, and the test shows an artificially increased storage modulus. Due to these properties, repeatability was very low for these samples, which made later analysis difficult as well.

The use of SPA also made the synthesis of the SHHs more complex by introducing another component. SPA somewhat improved the mechanical stiffness of the hydrogel, but a similar stiffness could be achieved by using higher concentrations of CNS. Additionally, SPA likely interfered with dissolution; the particles of SPA would not dissolve, which greatly impeded attempts to improve hydrogel dissolution. In particular, the anionic charge of SPA interacted with PAM's cationic charge and inhibited fast dissolution. Overall, the detriments that SPA introduced were more significant than its benefits, and the component was removed. None of the samples presented in the rest of this thesis contain SPA as a component; the appendix does contain tables with results including SPA.

4.5 Properties of CNS Suspension and Effect of CB[7] in Absence of Polymer

We analyzed the mechanical properties of CNS suspensions either alone or with CB[7] added to serve as a baseline. These experiments also offered insight into interaction among CNS sheets, and between CNS and CB[7]. As seen in Figure 4.13, rheometer testing shows a simple upward trend in storage modulus when increasing CNS concentrations, implying that the higher the concentration of CNS, the more structurally robust and rigid the sample becomes. When CB[7] is added to the SHH, there is a significant increase in storage modulus, though this increase becomes less substantial as CNS concentration increases.

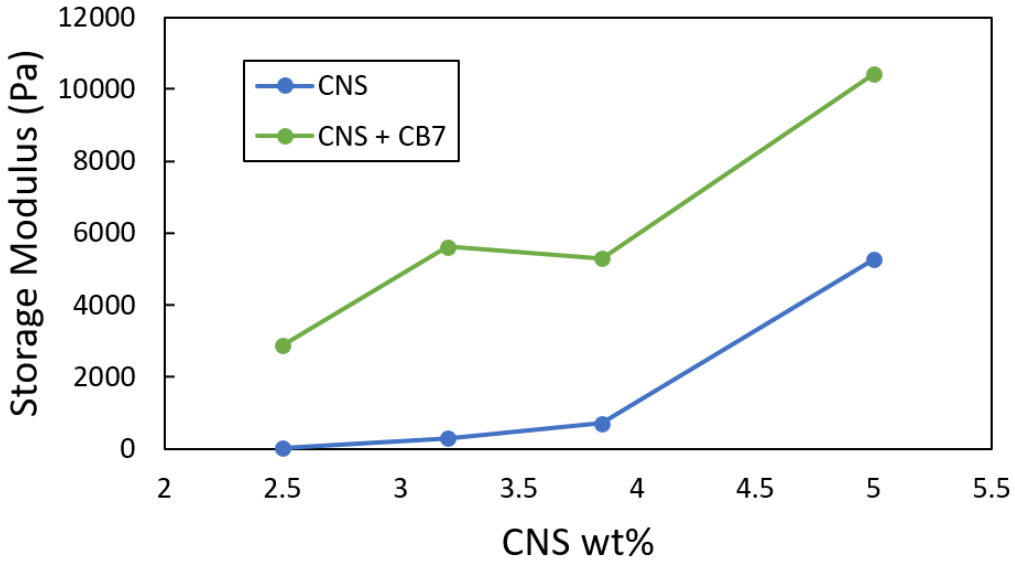

Figure 4.13: Storage modulus of CNS alone and CNS with 0.26 wt% CB[7]. CNS was tested at concentrations of 2.5, 3.2, 3.9, and 5 wt%. Storage modulus increases with the addition of CB[7] and at higher concentrations of CNS.

4.6 Effect of CNS Concentration on Mechanical Properties with Different Polymers

A major investigation of this thesis was the effect of different concentrations of CNS. We initially assumed that CNS was a simple component that acted mostly as a filler and that increasing CNS concentration would always lead to a stiffer hydrogel. However, this was not the case, particularly for PAM-based hydrogels. This section investigates the relation between CNS wt% and the storage modulus of the hydrogel. Concentrations of 2.5, 3.2, 3.9, and 5 CNS wt% were tested.

In SHHs formed with PMPC, as the CNS concentration increased, the storage modulus also rose, from 1000 to 6970 Pa, as seen in Figure 4.14. This behavior is consistent with a simple filler. This implies that there is very little interaction between PMPC and CNS, so the increased concentration of CNS does not interfere with any interactions between PMPC and CB[7]. Because CNS acts as a filler, the optimal hydrogel composition for PMPC is one with the highest CNS weight

percentage. The highest in this study was 5 wt%, due to solubility challenges for compounds like CB[7] and CNS. Here, the PMPC-based hydrogel is prepared in the default method of mixing with CNS and CB[7] mixed first, and PMPC added last.

In SHHs formed with PAM, there were deviations from the expected filler behavior. As seen in Figure 4.14, the storage modulus shows a non-monotonic correlation at varying CNS concentrations. This behavior implies that CNS and PAM interact. Initial addition of CNS strengthens the gels. However, above a certain concentration, CNS-PAM interactions begin to interfere with interactions between PAM and CB[7]. The optimal concentration for these electrostatic interactions in regard to storage modulus is with a CNS weight percentage of about 3.2 wt%.

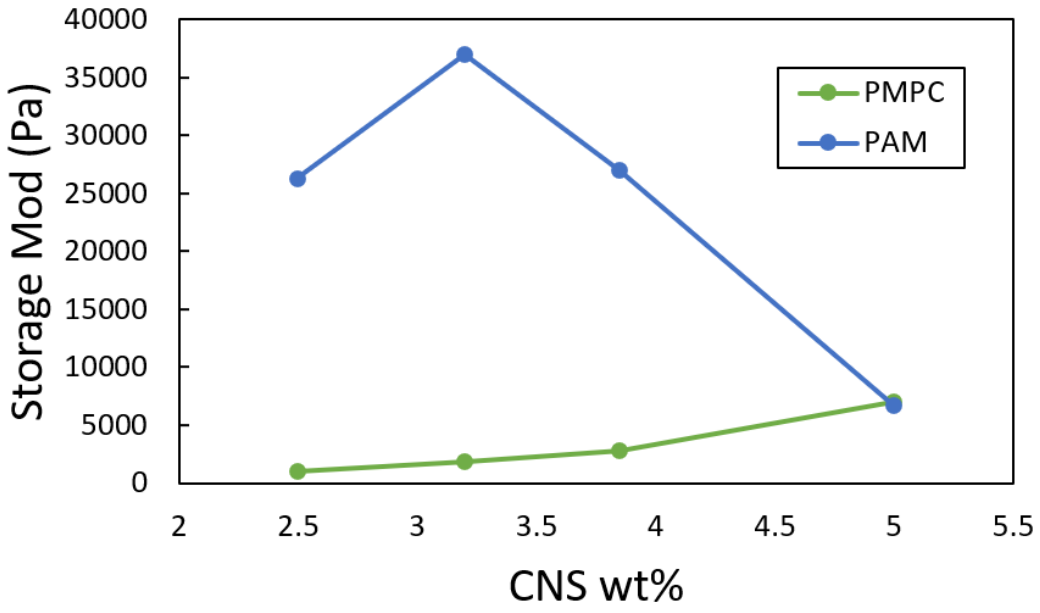

Figure 4.14: Storage modulus of hydrogels formed with PMPC and PAM, at 0.25 wt% polymer, 0.26 wt% CB[7], with 2.5, 3.2, 3.9, and 5 wt% of CNS. PMPC-based hydrogels show a gradual increase in storage modulus as CNS concentration increases, while PAM-based hydrogels show a peak at 3.2 wt% CNS.

4.7 Effect of CB[7] on Mechanical Properties with Different Polymers

While CB[7] is the main component intended to form supramolecular cross-links, as seen in Section 4.5, even samples without CB[7] can exhibit gelation due to polymer-CNS interactions as well as the assembly of CNS into a percolated network. Nonetheless, the addition of CB[7] allows for stronger, non-covalent electrostatic interactions to form between components, and produced a significant increase in mechanical properties. The increase in stiffness varied between polymers and CNS concentrations. The inclusion of 0.26 wt% CB[7], 0.25 wt% PMPC, and 2.5 - 5 wt% CNS led to a 9 times increase in storage modulus, with the advantage decreasing as CNS concentration increased, as seen in Figure 4.15 (top). Hydrogels incorporating PAM exhibited up to 10 times increase in storage modulus when CB[7] was included, with this advantage also decreasing as CNS concentrations increased, as Figure 4.15 (bottom) shows.

4.8 Effect of CB[7] Concentration on Mechanical Properties with Different Polymers

The effect of varying CB[7] concentration was investigated, looking at two different polymer concentrations with a constant CNS concentration of 3.2 wt%. This inquiry can help explain how and in what arrangements the polymer interacts with CB[7]. NMR analysis (see Section 4.2) shows that both PMPC and PAM have significant interactions with CB[7]. Testing of PAM-based hydrogels also shows that multiple monomer units may interact with the CB[7] ring, in various arrangements. Therefore, it was prudent to investigate how the ratio of CB[7] to polymer unit affected the mechanical properties of the hydrogels. This has been graphed below in Figure 4.16 as storage modulus versus the ratio between moles of CB[7] and moles of amine groups, which is the specific group interacting with CB[7]. For PMPC, this is each MPC monomer, while for PAM, the final synthesized polymer contained 46%

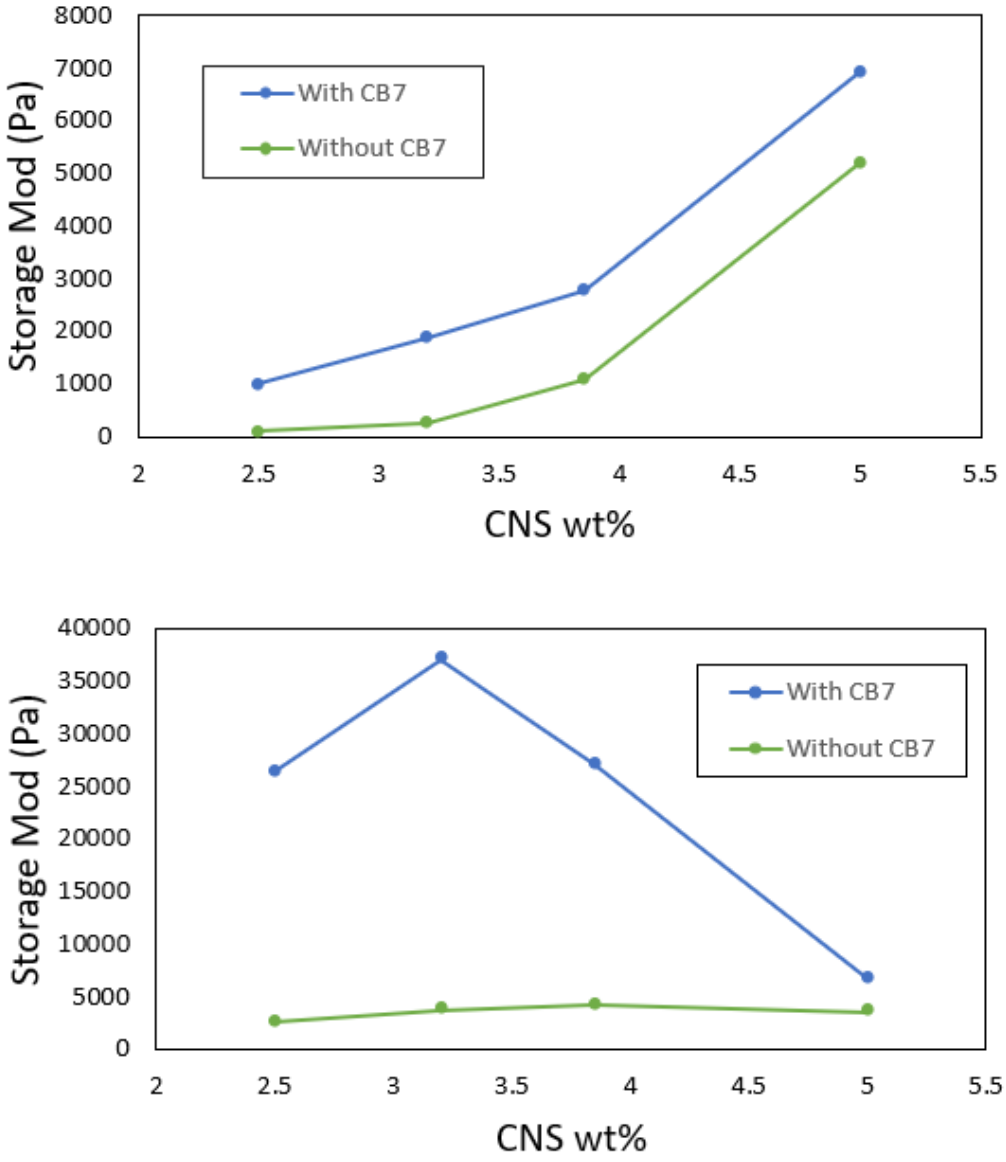

Figure 4.15: Storage modulus of PMPC (top) and PAM (bottom) with and without CB[7]. Tested at 0.25 wt% polymer and 0.26 wt% CB[7] (if included), with CNS at 2.5, 3.2, 3.9, and 5 wt%. Both show a significant increase in storage modulus with the addition of CB[7], with the most impressive increase occurring at lower concentrations of CNS.

MATMAC monomer (Gokaltun, 2023).

The storage modulus for PMPC-based hydrogels shows some variance with the ratio between moles of CB[7] and moles of polymer amine groups, as seen in Figure

4.16 (top). There is a general upwards trend as this ratio increases. The increase between 0.26 and 0.52 wt% CB[7] shows that the hydrogels perform better when there is around one CB[7] unit for every 2 MPC units as compared to one CB[7] for every 4 MPC units. This also suggests that higher ratios of CB[7] to amine group could result in better mechanical performance. This was outside of the scope of this thesis, mostly due to solubility challenges, but would be interesting to pursue in the future. Additionally, for the same CB[7] to amine group ratio, an increase in polymer concentration leads to stronger hydrogels.

When plotted against the CB[7]/Amine-group ratio, the storage modulus of PAM-based hydrogels exhibits a peak, as seen in Figure 4.16 (bottom), with the location of the peak depending on polymer concentration. These peaks correspond with the same ratio between CB[7] and CNS, with 0.26 wt% CB[7] and 3.2 wt% CNS. This aligns with previous suggestions that PAM has strong interactions with CNS. But with a minute amount of CB[7] present, CNS will over-occupy PAM and reduce its ability to interact with CB[7], resulting in a lower modulus. Then, as CB[7] concentration increases, cross-linking between CB[7] and PAM increases and we see an increase in modulus. But as CB[7] increases further, the amine groups get over-occupied by CB[7], which leads to more one-to-one interactions as the polymer gets end-capped by CB[7] instead of forming stronger cross-links. At the same time, CNS is interacting with both CB[7] and PAM, so the two are competing for those interactions. At a lower polymer concentration, there is less polymer available, so it takes more CB[7] to coat CNS before an ideal ratio is reached and there is a peak in storage modulus of the hydrogel. At a higher polymer concentration, there is more polymer available to interact with CNS, so less CB[7] is required and this peak occurs earlier.

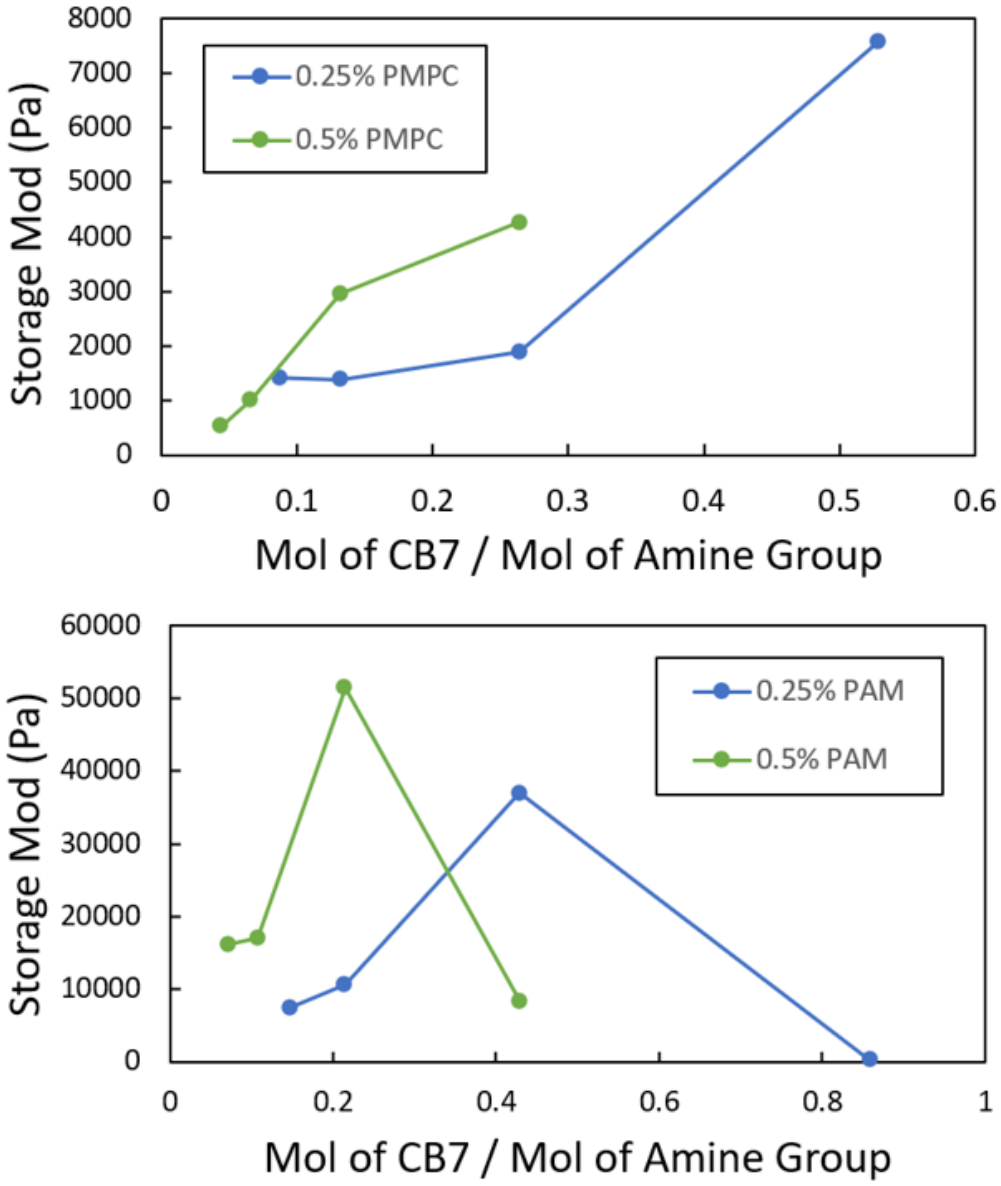

Figure 4.16: Storage modulus of PMPC (top) and PAM (bottom), at 3.2 wt% CNS and either 0.25 or 0.5 wt% polymer. CB[7] is varied from 0.086, 0.13, 0.26, and 0.52 wt%, represented here as a ratio between moles of CB[7] and moles of the polymer's amine group. With PMPC, an increase in CB[7] concentration leads to an increase in hydrogel storage modulus; with PAM, the hydrogel experiences a peak in storage modulus which is dependent on polymer concentration.

4.9 Effect of Mixing Order on Mechanical Properties of PMPC Hydrogels

We discovered that PMPC-based hydrogels displayed different mechanical properties depending on the order in which each component was mixed and explored these

phenomena further. When SPA is used as a component, the hydrogels for both polymers show no change in properties based on mixing order. However, without SPA, the behavior changes drastically for PMPC-based hydrogels depending on mixing order. No changes were observed for PAM-based hydrogels.

The default preparation method in this thesis is for CB[7] and CNS to be mixed initially, with PMPC added after. However, upon switching the order, with PMPC and CNS mixing first and then adding CB[7], PMPC-based hydrogels shows a marked increase in storage modulus and a non-monotonic distribution, seen clearly in Figure 4.17.

The reason for this is that PMPC doesn't interact strongly with CNS, but CB[7] does. When CB[7] is added to a CNS solution, it binds with CNS. When PMPC is added, there is little available CB[7] available to create cross-links between polymer chains. In contrast, when CB[7] is added to a mixture of CNS and PMPC, it can cross-link both components together, creating a stronger hydrogel. With PMPC and CNS added first, the storage moduli of the hydrogels now show a similar trend to those formed with PAM, where it encounters a peak at a given CNS concentration. Lower concentrations of CNS are not enough to provide structure for the electrostatic interactions, and too high a concentration begins to interfere with the interactions between PMPC and CB[7]. Using this preparation method, PMPC-based hydrogels show an optimal concentration of around 3.85 wt% CNS, slightly higher than hydrogels formed with PAM, which is at 3.2 wt%. At 3.85 wt%, PMPC-based hydrogels prepared in this order have a storage modulus over 3 times that of PMPC-based hydrogels prepared using the default mixing order.

The reason that PAM-based hydrogels show no change regarding mixing order is likely that both PAM and CB[7] interact with CNS, so changing which goes first does not affect the cross-linked structure as much.

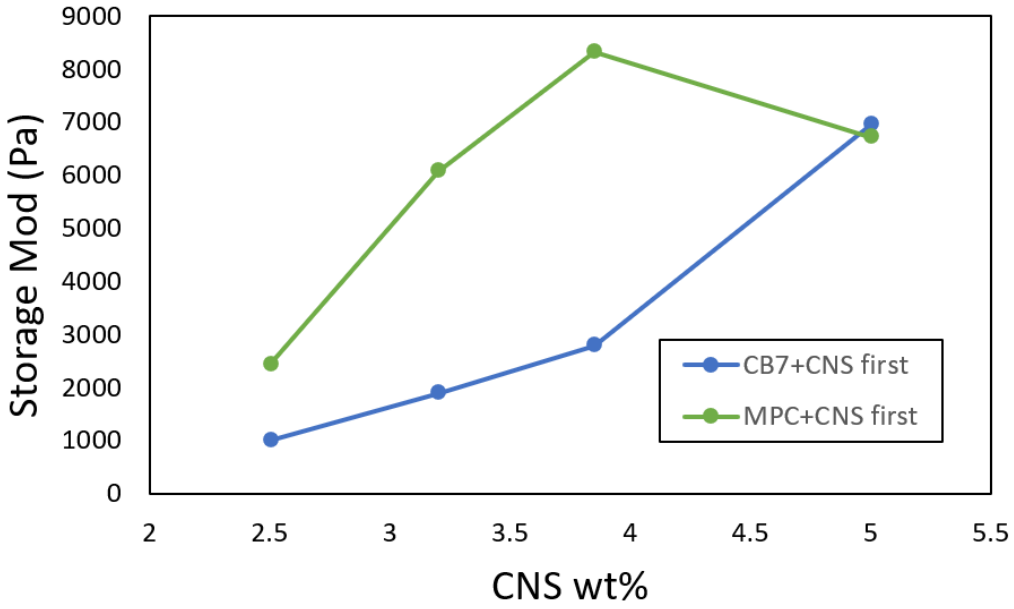

Figure 4.17: Storage modulus of PMPC using different preparation methods. The SHHs were prepared with 0.25 wt% polymer, 0.26 wt% CB[7], and 2.5, 3.2, 3.9, or 5 wt% CNS. When CB[7] and CNS are added before the polymer, the hydrogel shows a regular increase in storage modulus as CNS concentration increases. When the order is reversed and MPC and CNS are added before CB[7], the storage modulus increases significantly and a peak is seen at 3.9 wt% CNS.

4.10 Hydrogel On-Demand Dissolution

Once the hydrogels were synthesized, dissolution was tested. On-demand dissolution occurs when the supramolecular interactions between the polymer and CB[7] are disturbed. This happens when a more competitive molecule is introduced and CB[7] preferentially interacts with it. Dissolution can happen either when the dissolution agent replaces the polymer as the guest in the host-guest interaction, or when the dissolution agent has stronger ionic interactions and causes CB[7] to disassociate from the polymer without forming another insertion complex.

Dissolution was performed in PBS, 40 mM AH, and DIW, as we were interested in testing a range of ionic strengths. Briefly, 0.1 g of each hydrogel placed on a Petri dish, 0.2 mL of the dissolution solution was added, and light tapping was performed with the bulb of a pipette. This tapping broke up the hydrogel and within

seconds it would dissolve into many tiny particles. Though some of the particles stayed visible, they were sufficiently integrated into the liquid so that the mixture could be pipetted, as seen in Figure 4.18. Figure 4.19 shows a wide array of

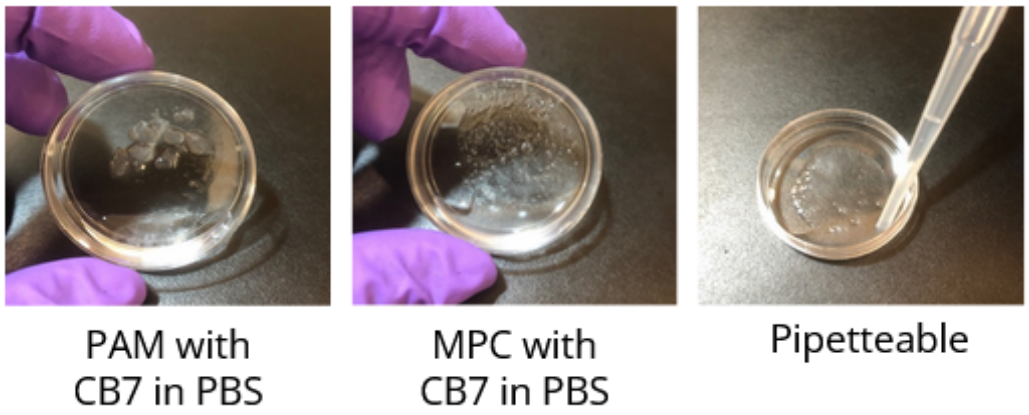

Figure 4.18: Dissolution testing in PBS, with SHHs formed from 0.25 wt% polymer, 0.26 wt% CB[7], and 3.2 wt% CNS. MPC-based hydrogels were prepared the in default order, with CB[7] and CNS added first. Both SHHs show dissolution, with only small, pipettable pieces remaining.

gels and how they dissolved in PBS using the method described above. Samples containing CB[7] dissolved more easily upon the addition of 0.2 mL PBS, as the particles separated quickly and were smaller. Hydrogels containing PMPC also showed a faster and more complete dissolution with PBS when compared to PAM hydrogels. This is likely due to the fact that PMPC doesn't interact strongly with CNS, so there are fewer bonds to break, as well as the overall neutral character of the PMPC monomer - compared to the positively charged PAM, PMPC does not have as strong an interaction with the charged sections of CB[7]. This means the interactions between PMPC units and CB[7] molecules can be disrupted more easily by high ionic strength solutions.

Figure 4.19 also shows that the inclusion of SPA greatly inhibits dissolution and can also be seen more clearly in Figure 4.20. SPA is a negatively charged polymer that bridges between CNS structures and works to retain the integrity of the hydrogel

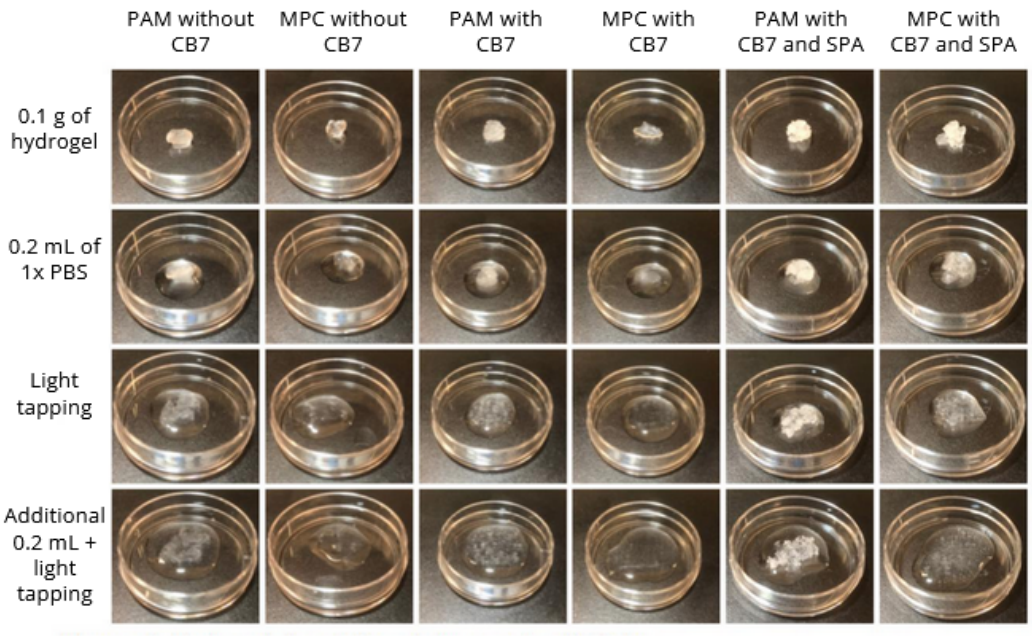

Figure 4.19: Dissolution testing array of various samples in PBS. SHHs without SPA were prepared with 0.25 wt% polymer, 0.26 wt% CB[7] (if included), and 3.2 wt% CNS. SHHs prepared with SPA contained 0.14 wt% SPA, 0.25 wt% polymer, 0.26 wt% CB[7], and 2 wt% CNS. SHH dissolution was most complete in hydrogels without SPA and with CB[7]; PMPC-based hydrogels also dissolved easier than those with PAM.

even at high ionic strength solutions. SPA has more significant effect when using PAM, which contains cationic charges. The hydrogel made with PAM and SPA did not dissolve like the other samples - it remained in one piece and separate from the dissolution solution. The effect of SPA on PMPC is not so drastic, but still prevented as complete a dissolution compared to samples not containing SPA. This dissolution testing was performed with PBS, DIW with AH (40 mM), and DIW alone, as seen in Figure 4.21. All solutions showed sufficient levels of dissolution, with PBS performing the best and DIW the worst, though it is difficult to quantify the process. Here, 0.1g of hydrogel was placed in 2 mL of the chosen dissolution solution, and pictures were taken after 1 minute. Both PMPC and PAM based hydrogels quickly dissolved in PBS with few particles remaining visible. For DIW + AH, the hydrogel experienced dissolution, but larger particles were still visible. For DIW alone, the

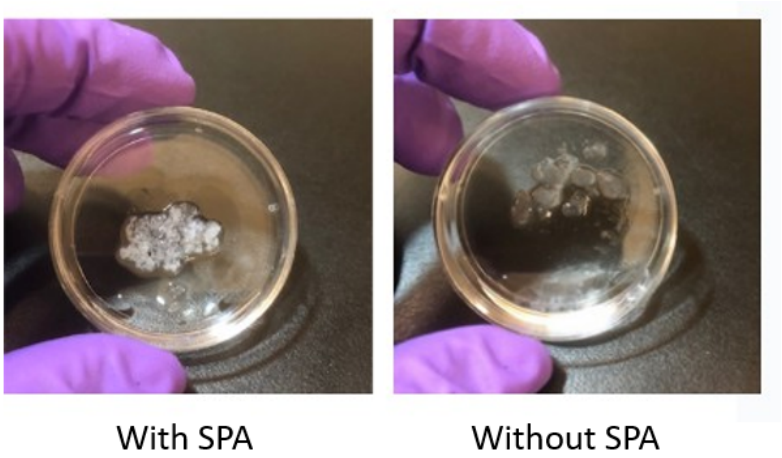

Figure 4.20: Dissolution of PAM-based hydrogels with and without SPA (left and right respectively). The SHH with SPA was prepared with 0.14 wt% SPA, 0.25 wt% PAM, 0.26 wt% CB[7], and 2 wt% CNS. The SHH without SPA contained 0.25 wt% PAM, 0.26 wt% CB[7], and 3.2 wt% CNS. SHHs without SPA experienced faster and more complete dissolution than those containing SPA.

hydrogel swelled but did not immediately break apart.

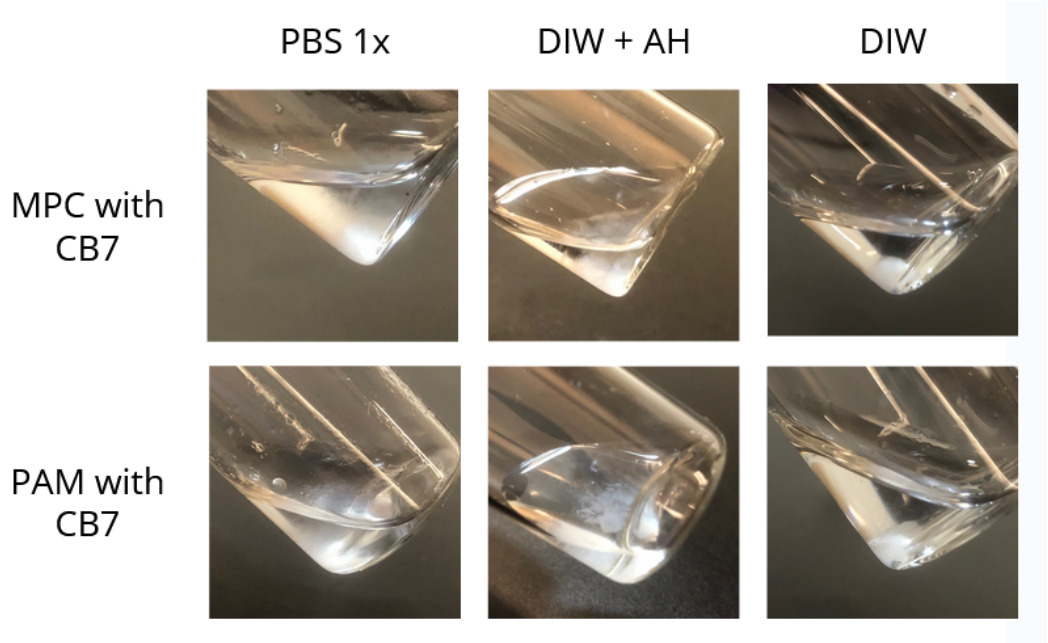

Figure 4.21: Dissolution of hydrogels in solutions of PBS, DIW+AH (40 mM), and DIW alone. Hydrogels were prepared with 0.25 wt% polymer, 0.26 wt% CB[7], and 3.2 wt% CNS. PBS was the most effective dissolution agent, but all resulted in some level of dissolution.

4.11 Use of Other Polymers in Hydrogel Formation

We wanted to understand the link between polymer structure for polymers containing positive charged groups and gel formation. The polymer PEI, polyethylenimine, was also considered; it's branched structure is shown in Figure 4.22. It is a cationic branched polymer, with an average Mw of 25,000 by LS and an average Mn of 10,000 by GPC. SHHs formed with PEI behaved very similarly to PMPC-based hydrogels, with a storage modulus of 2200 Pa with 0.26 wt% CB[7] and 3.2 wt% CNS. As can be seen farther below in Figure 4.24 (top), the addition of CB[7] increased its storage modulus by about 2 times, showing that there are interactions between the two components, though they were not as significant as PAM or PMPC. We also considered the polymer PMM+, or poly (methyl methacrylate-*random*-

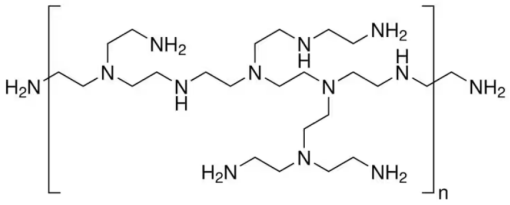

Figure 4.22: Branched PEI chemical structure.

3-(methacryloylamino) propyl trimethylammonium chloride) (MMA-r-MATMAC, called PMM+). It's chemical structure is shown in Figure 4.23. It was synthesized following a free radical polymerization. SHHs made with PMM+ behaved very similarly to PAM-based hydrogels, with a storage modulus of 23500 Pa with 0.26 wt% CB[7] and 3.2 wt% CNS. The addition of CB[7] increased its storage modulus by about 5 times, seen in Figure 4.24 (bottom), showing that CB[7] and PMM+ do indeed interact.

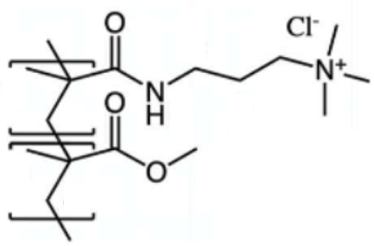

Figure 4.23: PMM+ chemical structure.

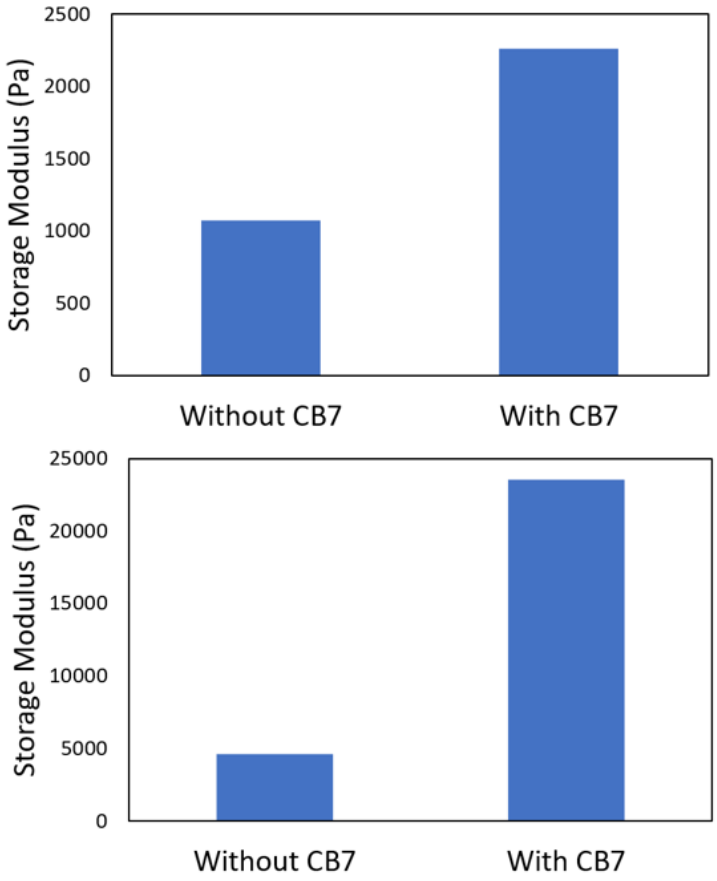

Figure 4.24: Storage modulus of PEI (top) and PMM+ (bottom) with and without CB[7]. SHHs were formed with 0.25 wt% polymer, 0.26 wt% CB[7] (if included), and 3.2 wt% CNS. Hydrogels with PMM+ were significantly stronger than those with PEI, but both showed impressive increases in storage modulus upon the addition of CB[7].

Chapter 5

CONCLUSION

This research confirms that SHHs made with PAM or PMPC form mechanically robust hydrogels that have potential applications in biomedical fields, particularly that of burn wound dressings. PAM-based hydrogels performed best in mechanical testing and had the best structural integrity, in agreement with previous work in the lab. PMPC-based hydrogels did not create as mechanically strong hydrogels, but the zwitterionic nature of the polymer lends it certain advantages. It is inert, highly hydrophilic, and fouling resistant due to its overall neutral charge (Liu, 2022). It also has impressively fast dissolution with PBS, AH, and DIW, and is biocompatible. Though less mechanically robust, it still meets our standards for a burn wound dressing.

It was also concluded that SPA should be eliminated as a component to improve homogeneity and dissolution properties. After removing SPA, any subsequent decrease in mechanical properties can be regained by increasing CNS concentrations. In SHHs formed with PAM, CNS interactions with both PAM and CB[7] can eventually interfere with the more significant interactions between just PAM and CB[7], so there is an upper limit on CNS wt%. The same is not true for PMPC-based hydrogels because CNS doesn't interact strongly, so CNS functions as a filler, showing a steady increase in stiffness as CNS concentrations rise. However, this changes when the mixing order of PMPC is changed from CNS and CB[7] first to instead CNS and PMPC first. We then see a non-monotonic distribution as well the interactions between CNS and CB[7] begin to inhibit mechanical properties when CNS concentrations are high enough, though the storage modulus increases overall. When varying CB[7] ratios, we see that at the same CB[7] concentration, higher

polymer wt% results in a stronger hydrogel. Storage modulus increases indicating increasing cross-linking density, but decreases at a certain CNS concentration as CNS over-occupies PAM and restricts its cross-linking density with CB[7] - there is an ideal ratio between CNS and CB[7] that sees the largest peak. They also exhibit on-demand dissolution in several solutions; we tested with PBS, AH, and DIW. With small movement applied, these hydrogels dissolve into a pipettable liquid within several seconds in PBS.

This research offers a better understanding of the interactions between components, resulting in the ideal SHH composition for both PAM and PMPC. The hydrogels produced with either of these polymers are within the bounds for a functional burn wound dressing material, displaying sufficient mechanical stiffness and ease of dissolution. Using such hydrogels for burn wound dressings can provide easy burn care and eliminate the need for debridement, which promotes the healing process. This will greatly benefit both patients and healthcare providers by reducing pain and reliance on opioids, dressing change time, hospital stay duration, and overall cost of treatment. Due to the ease of fabrication, consisting of three components, these hydrogels can also be easily scaled-up to produce large-scale but low-cost dressings. Additionally, due to the speed of formation, these SHHs could also be synthesized at the bedside or by first responders in-field. With future customization, these SHHs can be antimicrobial, which will further enhance healing for second-degree burns.

These SHHs also have use in applications outside of just burn wound dressings, and may find other uses in the broad field of biomedical engineering. The ease of formation, mechanical stiffness and quick dissolution are all useful properties in tissue and micro-tissue engineering, biopreservation, drug delivery, and cell scaffolding for imaging or 3D printing. The zwitterionic properties of PMPC are also valuable for self-healing and anti-fouling applications.

Chapter 6

FUTURE WORK

In the future, further testing of a greater array of hydrogels would strengthen the work of this thesis. This thesis only tested up to 5 wt% CNS due to solubility limitations. It would be informative to increase the concentration and see if PMPC-based hydrogels reach an upper limit and level out or drop considerably, like PAM-based hydrogels do at 3.2 wt% CNS. Also, it would be interesting to see how hydrogels perform at higher concentrations of polymer. This work only went up to 0.5 wt% polymer, which is very small compared to other components. Dramatically increasing the polymer concentration could have interesting effects. To keep the polymer:CB[7] ratios the same would mean increasing the amount of CB[7], which can be expensive, and is thus why this thesis focused on smaller quantities.

It would also be beneficial to expand the types of materials tested. Only PAM and PMPC were seriously investigated, although PEI and PMM+ showed promise. It would be prudent to experiment more with these polymers and see how they interact with different concentrations of CNS. It would also be very interesting to combine PAM and PMPC and observe which behaviors prevail. The addition of a zwitterionic polymer to the stronger PAM hydrogel may result in a higher storage modulus but easier dissolution. Additionally, future work could look at "hosts" other than CB[7], such as cyclodextrins or tannic acid. CB[7] is very expensive and difficult to obtain - if other host chemicals perform similarly, then it could greatly reduce the cost and supply acquisition time.

There can also be further investigation into the effect of changing the mixing order of PMPC-based hydrogels and the underlying mechanisms that produce the change in storage modulus. It was only tested at one concentration of PMPC and CB[7] - at

different ratios, is the storage modulus affected the same as with the standard mixing order? Additionally, the polymer PEI had a similar storage modulus as PMPC-based hydrogels - would changing the mixing order for PEI have a similar effect?

There are several material characterization techniques that would also be beneficial to this work. We did not investigate dehydration or swelling of the hydrogels, or their pH stability or self-healing ability. Previous work on these hydrogels have performed some of these tests but including SPA. It is unknown how the removal of SPA would affect these properties (Gokaltun, 2023).

The next step for making these hydrogels even more efficient at burn wound healing would be to incorporate antimicrobials, such as silver nanoparticles. It's also necessary to create an efficient application process for these hydrogels that allows for easy mixing, such as an applicator tool. A functional applicator would also allow for better scale-up testing, such as using molds. Additionally, further biological testing is needed. Previous work has evaluated *in vitro* and *in vivo* biocompatibility of SHHs. The SHH demonstrates excellent biocompatibility in both *in vitro* testing with human cells and *in vivo* murine implanation experiments (Gokaltun, 2023). The next step would be swine testing to ensure it functions as predicted for burn healing.

BIBLIOGRAPHY

Ahmed, Enas (2015). "Hydrogel: Preparation, characterization, and applications: A review". In: *Journal of Advanced Research* 6 (2), pp. 105–121.

Asatekin, Ayse (2023). "Supramolecular hybrid hydrogels for burn and wound dressings". In: *US Patent FH Application FH11515315.3*.

Barrow, Steven (2015). "Cucurbituril-Based Molecular Recognition". In: *ACS Publications: Chemical Reviews* 115, pp. 12320–12406.

Celik, Enes (2023). "Is hydrogel burn dressing effective on burn pain?" In: *Burns*.

Choinière, Manon (1989). "The Pain of Burns: Characteristics and Correlates". In: *Journal of Trauma and Acute Care Surgery* 29 (11), pp. 1531–1539.

Council, National Safety (2023). *Deaths by Demographics - Top 10 Preventable Injuries*. URL: https://injuryfacts.nsc.org/all-injuries/deaths-by-demographics/top-10-preventable-injuries/data-details/.

Duchin, Emma (2021). "Burn patients' pain experiences and perceptions". In: *Burns* 47 (7), pp. 1627–1634.

Evans, Christopher (2022). "Burn related injuries: a nationwide analysis of adult inter-facility transfers over a six-year period in the United States". In: *BMC Emergency Medicine* 22 (147).

Gokaltun, Aslihan (2023). "Supramolecular hybrid hydrogels as rapidly on-demand dissoluble, self-healing, and biocompatible burn dressings". In: *Bioactive Materials* 25, pp. 415–429.

Harada, Akira (2015). "Supramolecular Hydrogels". In: *Encyclopedia of Polymeric Nanomaterials*, pp. 2372–2377.

Holt, Brian (2008). “Viscoelastic Response of Human Skin to Low Magnitude Physiologically Relevant Shear”. In: *Journal of Biomechanics* 41 (12), pp. 2689–2695.

Hop, M (2014). “Costs of burn care: A systematic review”. In: *Wound Repair and Regeneration* 22, pp. 436–450.

James, Dominika Lipowska (2017). “Principles of Burn Pain Management”. In: *Clinics in Plastic Surgery* 44 (4), pp. 737–747.

Kalra, Anubha (2016). “Mechanical Behaviour of Skin: A Review”. In: *Journal of Material Science & Engineering* 5 (4).

Kearney, Steven (2015). “Dynamic viscoelastic models of human skin using optical elastography”. In: *Physics in Medicine & Biology* 60 (17), p. 6975.

Konieczynska, Marlena D. (2016). “On-Demand Dissolution of a Dendritic Hydrogel-based Dressing for Second-Degree Burn Wounds through Thiol–Thioester Exchange Reaction”. In: *Angewandte Chemie International Edition* 55 (34), pp. 9984–9987.

Latarjet, J (1995). “Pain in Burn Patients”. In: *Burns* 21 (5), pp. 344–348.

Liu, Sihang (2022). “Recent Advances in Zwitterionic Hydrogels: Preparation, Property, and Biomedical Application”. In: *Gels* 8 (46).

Mosier, Michael (2016). *National Burn Repository*. Tech. rep. American Burn Association.

Omar, Jasmin (2022). “Supramolecular Hydrogels: Design Strategies and Contemporary Biomedical Applications”. In: *Chemistry: An Asian Journal* 17 (9).

Opriessnig, Elisa (2023). “Epidemiology of burn injury and the ideal dressing in global burn care – Regional differences explored”. In: *Burns* 49 (1), pp. 1–14.

Peck, Michael (2011). “Epidemiology of burns throughout the world. Part I: Distribution and risk factors”. In: *Burns* 37 (7), pp. 1087–1100.

Selig, Harald (2012). “The properties of an “ideal” burn wound dressing – What do we need in daily clinical practice? Results of a worldwide online survey among burn care specialists”. In: *Burns* 38 (7), pp. 960–966.

Siavash, Mansour (2023). “The Ideal Wound Dressing”. Online Preprint.

Silver, Frederick (2002). “Viscoelastic Properties of Young and Old Human Dermis: A Proposed Molecular Mechanism for Elastic Energy Storage in Collagen and Elastin”. In: *Journal of Applied Polymer Science* 86, pp. 1978–1985.

Tomas, Helena (2018). “Laponite®: A key nanoplatform for biomedical applications?” In: *Nanomedicine: Nanotechnology, Biology and Medicine* 14 (7), pp. 2407–2420.

Wang, Wenda (2020). *Polymer Science and Nanotechnology: Fundamentals and Applications*. Elsevier. Chap. 10, pp. 203–244.

Wasiak, Jason (2013). “Dressings for superficial and partial thickness burns”.

Williams, Felicia N (2009). “The leading causes of death after burn injury in a single pediatric burn center”. In: *Critical Care* 13 (6).

Xu, Wenwen (2017). “Supramolecular Hydrogels Fabricated from Supramonomers: A Novel Wound Dressing Material”. In: *ACS Applied Materials & Interfaces* 9 (13), pp. 11368–11372.

Yu, Tzy-Chyi (2020). “Healthcare resource utilization, treatment patterns, and cost of care among patients with thermal burns and inpatient autografting in two large privately insured populations in the United States”. In: *Burns* 46 (4), pp. 825–835.

Appendix A

SUPPORTING INFO

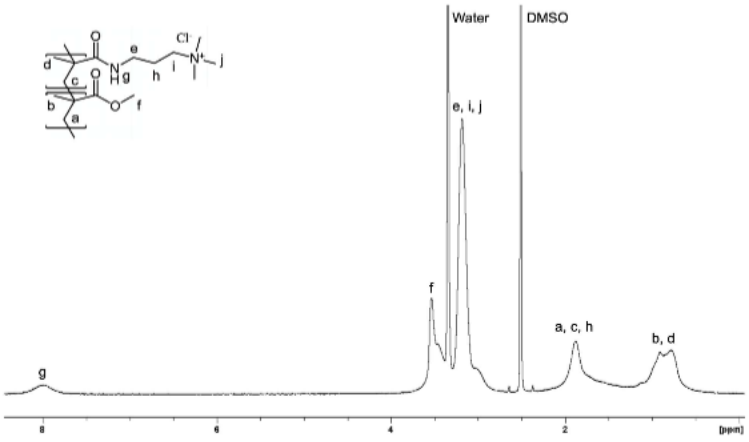

Figure A.1: ^{1}H NMR of PAM.

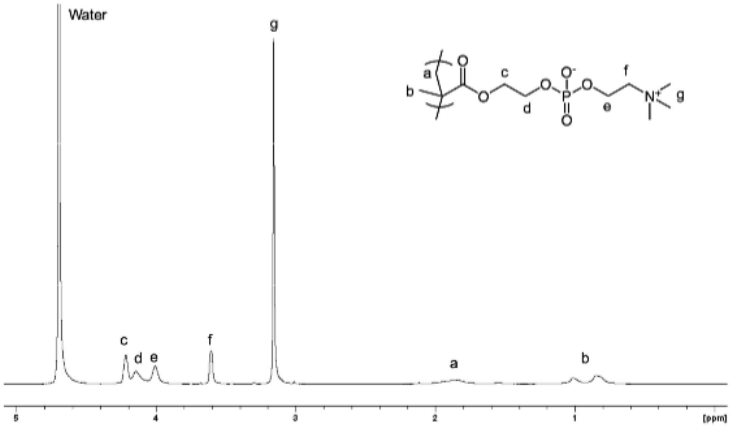

Figure A.2: ^{1}H NMR of MPC.

Appendix B

SELECTED RHEOMETER GRAPHS

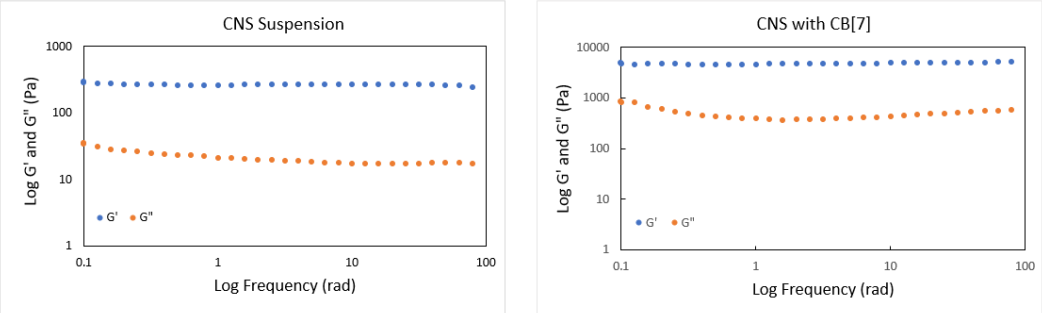

Figure B.1: Storage (G') and loss (G") moduli of pure CNS suspension (left) and CNS with CB[7] (right). Gels contain 3.2 wt% CNS, and 0.26 wt% CB[7] (if included).

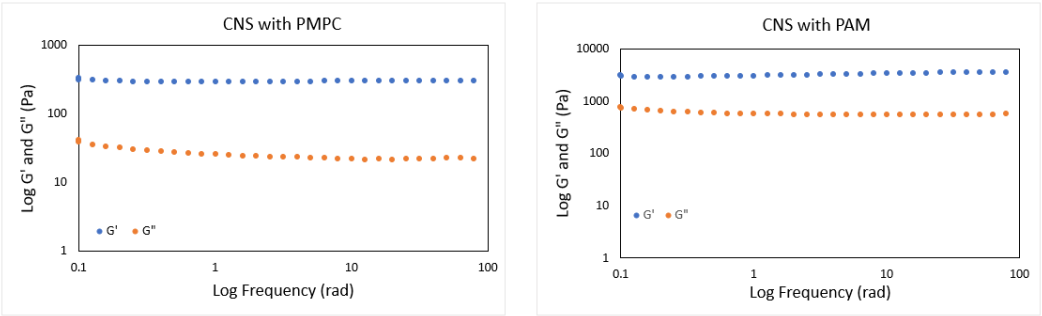

Figure B.2: Storage (G') and loss (G") moduli of CNS with PMPC (left) and CNS with PAM (right). Gels contain 3.2 wt% CNS, and 0.25 wt% polymer.

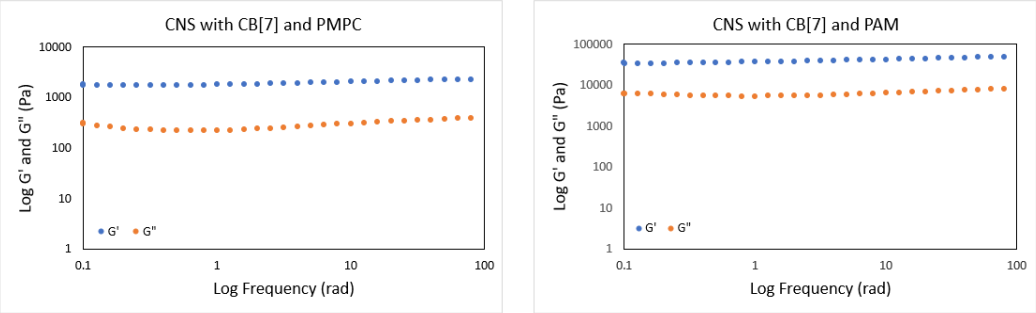

Figure B.3: Storage (G') and loss (G") moduli of CNS with CB[7] and PMPC (left) and CNS with CB[7] and PAM (right). Gels contain 3.2 wt% CNS, 0.26 wt% CB[7], and 0.25 wt% polymer.

Appendix C

SHH COMPOSITION TABLE: CONTROLS

Table C.1: Control Samples.

Sample #	**CNS (wt%, mL)**		**CB[7] (wt%, mL)**		**SPA (wt%, mL)**		**DIW (mL)**
	Conc in Stock Solution	Vol of Stock Solution	Conc in Stock Solution	Vol of Stock Solution	Conc in Stock Solution	Vol of Stock Solution	Vol of Stock Solution
Control-2	5%	1	0	0	0	0	1
Control-3	5%	1.28	0	0	0	0	0.72
Control-4	5%	1.54	0	0	0	0	0.46
Control-5	4%	1.6	2%	0.26	0	0	0.14

Appendix D

SHH COMPOSITION TABLE: PAM

Table D.1: PAM Samples.

Sample #	**PAM (wt%, mL)**		**CNS (wt%, mL)**		**CB[7] (wt%, mL)**		**DIW (mL)**
	Conc in Stock Solution	Vol of Stock Solution	Conc in Stock Solution	Vol of Stock Solution	Conc in Stock Solution	Vol of Stock Solution	Vol of Stock Solution
Control-7	2.5%	0.2	5%	1	0	0	0.8
Control-8	2.5%	0.2	5%	1.28	0	0	0.52
Control-9	2.5%	0.2	5%	1.54	0	0	0.26
Control-10	2.5%	0.4	5%	1	0	0	0.6
Control-11	2.5%	0.4	5%	1.28	0	0	0.32
Control-12	2.5%	0.4	5%	1.54	0	0	0.06
Control-13	5%	0.1	6%	1.64	0	0	0.26
SHH-13	2.5%	0.2	5%	1.28	2%	0.26	0.26
SHH-14	2.5%	0.2	5%	1.54	2%	0.26	0

Continued on next page

Table D.1 – continued from previous page

Sample #	PAM (wt%, mL)		CNS (wt%, mL)		CB[7] (wt%, mL)		DIW (mL)
SHH-15	2.5%	0.2	4%	1.25	2%	0.26	0.29
SHH-16	2.0%	0.4	5%	1	2%	0.26	0.34
SHH-17	2.5%	0.4	5%	1.28	2%	0.26	0.06
SHH-18	2.5%	0.4	5.8%	1.328	2%	0.26	0.012
SHH-19	2.5%	0.4	5.8%	1.103	2%	0.5	0
SHH-20	2.5%	0.2	5%	1.28	2%	0.13	0.39
SHH-21	2.5%	0.2	5%	1.28	2%	0.087	0.433
SHH-22	5%	0.1	6%	1.64	2%	0.26	0
SHH-23	2.5%	0.2	5%	1.28	2%	0.26	0.26
SHH-24	2.5%	0.2	5.8%	1.54	2%	0.26	0
SHH-25	2.5%	0.4	6%	1.067	2%	0.13	0.403
SHH-26	2.5%	0.4	6%	1.067	2%	0.087	0.446
SHH-27	2.5%	0.2	6%	1.067	2%	0.52	0.213

Appendix E

SHH COMPOSITION TABLE: PMPC

Table E.1: PMCP Samples.

Sample #	**PAM (wt%, mL)**		**CNS (wt%, mL)**		**CB[7] (wt%, mL)**		**SPA (wt%, mL)**		**DIW (mL)**
	Conc in Stock Solution	Vol of Stock Solution	Conc in Stock Solution	Vol of Stock Solution	Conc in Stock Solution	Vol of Stock Solution	Conc in Stock Solution	Vol of Stock Solution	Vol of Stock Solution
Control-14	2.4%	0.21	4%	1	0	0	0.28%	1	0
Control-15	2.5%	0.2	5%	1	0	0	0	0	0.8
Control-16	2.5%	0.2	5%	1.54	0	0	0	0	0.52
Control-17	2.5%	0.2	5%	1.54	0	0	0	0	0.26

Continued on next page

Table E.1 – continued from previous page

Sample #	PAM (wt%, mL)		CNS (wt%, mL)		CB[7] (wt%, mL)		SPA (wt%, mL)		DIW (mL)
Control-18	2.5%	0.4	5%	1	0	0	0	0	0.6
Control-19	2.5%	0.4	5%	1.28	0	0	0	0	0.32
Control-20	2.5%	0.4	5%	1.54	0	0	0	0	0.06
Control-21	2.5%	0.2	4%	1	0	0	0	0	0.8
Control-22	2.5%	0.2	4%	1.8	0	0	0	0	0
Control-23	5%	0.1	6%	1.64	0	0	0	0	0.26
SHH-28	2.5%	0.2	4%	1	2.6%	0.2	0.56%	0.5	0.1
SHH-29	2.5%	0.2	5%	1.28	2%	0.26	0	0	0.26

Continued on next page

Table E.1 – continued from previous page

Sample #	PAM (wt%, mL)		CNS (wt%, mL)		CB[7] (wt%, mL)		SPA (wt%, mL)		DIW (mL)
SHH-30	2.5%	0.2	5%	1.54	2%	0.26	0	0	0
SHH-31	2.5%	0.2	4%	1.25	2%	0.26	0	0	0.29
SHH-32	2.5%	0.4	5%	1	2%	0.26	0	0	0.34
SHH-33	2.5%	0.4	5%	1.28	2%	0.26	0	0	0.06
SHH-34	2.5%	0.4	5.8%	1.33	2%	0.26	0	0	0.012
SHH-35	2.5%	0.4	5.8%	1.103	2%	0.5	0	0	0
SHH-36	2.5%	0.2	5.8%	1.54	2%	0.26	0	0	0
SHH-37	2.5%	0.2	5%	1.28	2%	0.13	0	0	0.39

Continued on next page

Table E.1 – continued from previous page

Sample #	PAM (wt%, mL)		CNS (wt%, mL)		CB[7] (wt%, mL)		SPA (wt%, mL)		DIW (mL)
SHH-38	2.5%	0.2	5%	1.28	2%	0.087	0	0	0.43
SHH-39	5%	0.1	6%	1.64	2%	0.26	0	0	0
SHH-40	2.50%	0.2	5%	1.28	2%	0.26	0	0	0.26
SHH-41	5%	0.1	6%	1.64	2%	0.26	0	0	0
SHH-42	2.50%	0.2	4%	1.25	2%	0.26	0	0	0.29
SHH-43	2.50%	0.2	6%	1.28	2%	0.26	0	0	0.26
SHH-44	2.50%	0.4	6%	1.07	2%	0.13	0	0	0.403
SHH-45	2.50%	0.4	6%	1.07	2%	0.087	0	0	0.446

Continued on next page

Table E.1 – continued from previous page

Sample #	**PAM (wt%, mL)**		**CNS (wt%, mL)**		**CB[7] (wt%, mL)**		**SPA (wt%, mL)**		**DIW (mL)**
SHH-46	2.50%	0.2	6%	1.07	2%	0.52	0	0	0.213
SHH-47	2.50%	0.2	5%	1.54	2%	0.26	0	0	0

Appendix F

SHH COMPOSITION TABLE: PEI & PMM+

Table F.1: PEI Samples.

Sample #	**PEI (wt%, mL)**		**CNS (wt%, mL)**		**CB[7] (wt%, mL)**		**SPA (wt%, mL)**		**DIW (mL)**
	Conc in Stock Solution	Vol of Stock Solution	Conc in Stock Solution	Vol of Stock Solution	Conc in Stock Solution	Vol of Stock Solution	Conc in Stock Solution	Vol of Stock Solution	Vol of Stock Solution
Control-24	2.4%	0.2	4%	1	0	0	0.28%	1	0
SHH-48	2.50%	0.2	5%	1.28	2%	0.26	0	0	0.26

Table F.2: PMM+ Samples.

Sample #	**PMM+ (wt%, mL)**		**CNS (wt%, mL)**		**CB[7] (wt%, mL)**		**SPA (wt%, mL)**		**DIW (mL)**
	Conc in Stock Solution	Vol of Stock Solution	Conc in Stock Solution	Vol of Stock Solution	Conc in Stock Solution	Vol of Stock Solution	Conc in Stock Solution	Vol of Stock Solution	Vol of Stock Solution
Control-25	2.40%	0.2	4%	1	0	0	0.28%	1	0
SHH-49	2.50%	0.2	5%	1.28	2%	0.26	0	0	0.26

Appendix G

SHH DATA TABLE: CONTROLS

Table G.1: Control Samples.

Sample #	**CNS (wt./v)**	**CB[7] (wt./v)**	**SPA (wt./v)**	**G'**	**G"**
	%	%	%	(Pa)	(Pa)
Control-1	2	0.26	0.14	N/A	N/A
Control-2	2.5	0	0	12.35 ± 4.90	5.14 ± 2.45
Control-3	3.2	0	0	290.1 ± 35.1	22.7 ± 1.78
Control-4	3.85	0	0	698.5 ± 13.4	39.47 ± 0.04
Control-5	3.2	0.26	0	4741.99 ± 319.37	475.15 ± 35.09

Appendix H

SHH DATA TABLE: PAM

Table H.1: PAM Samples.

Sample #	**CNS (wt./v)**	**CB[7] (wt./v)**	**SPA (wt./v)**	**PAM (wt./v)**	**G'**	**G"**
	‰	‰	‰	‰	(Pa)	(Pa)
Control-6	2	0	0.14	0.25	3400 ± 556.7	600 ± 132.6
Control-7	2.5	0	0	0.25	2524.21	336.99
Control-8	3.2	0	0	0.25	3720.1 ± 760.1	725.79 ± 195.9
Control-9	3.85	0	0	0.25	4189.5 ± 221.2	550.84 ± 17.24
Control-10	2.5	0	0	0.5	4404.4 ± 576.5	933.00 ± 120.4
Control-11	3.2	0	0	0.5	5471.7 ± 430.3	1015.265 ± 34.24

Continued on next page

Table H.1 – continued from previous page

Sample #	**CNS (wt./v)**	**CB[7] (wt./v)**	**SPA (wt./v)**	**PAM (wt./v)**	**G'**	**G''**
Control-12	3.85	0	0	0.5	7230.4 ± 506.0	982.89 ± 118.5
Control-13	5	0	0	0.25	3521.86 ± 173.41	441.65 ± 27.57
SHH-1	2	0.26	0.06	0.15	3500 ± 791.4	500 ± 117.5
SHH-2	2	0.26	0.1	0.15	8700 ± 571.7	1200 ± 74.9
SHH-3	2	0.26	0.14	0.15	19000 ± 1297.7	2700 ± 227.7
SHH-4	2	0.26	0.14	0.25	50000 ± 6756.6	7700 ± 657.6
SHH-5	2	0.26	0	0.25	18000 ± 2135.5	3200 ± 416.5
SHH-6	2	0.26	0.14	0.5	27000 ± 3657.9	4100 ± 550.6

Continued on next page

Table H.1 – continued from previous page

Sample #	**CNS (wt./v)**	**CB[7] (wt./v)**	**SPA (wt./v)**	**PAM (wt./v)**	**G'**	**G"**
SHH-7	2	0.52	0.14	0.5	1700 ± 70.9	200 ± 4.0
SHH-8	2.5	0.26	0.14	0.25	12000 ± 1768.3	1700 ± 237.7
SHH-9	3	0.26	0.14	0.5	24000 ± 1056.2	3800 ± 40.5
SHH-10	4	0.26	0.14	0.5	26000 ± 1797.2	4300 ± 341.3
SHH-11	3	0.26	0.14	0.25	13000 ± 1460.6	2100 ± 249.5
SHH-12	4	0.26	0.14	0.25	8800 ± 704.1	1400 ± 119.5
SHH-13	3.2	0.26	0	0.25	37005.2 ± 4017.38	5964.1 ± 407.62
SHH-14	3.85	0.26	0	0.25	27018.7 ± 4299.95	4757.45 ± 739.59

Continued on next page

Table H.1 – continued from previous page

Sample #	**CNS (wt./v)**	**CB[7] (wt./v)**	**SPA (wt./v)**	**PAM (wt./v)**	**G'**	**G''**
SHH-15	2.5	0.26	0	0.25	40330.7 ± 19845.0	6701.17 ± 2881.6
SHH-16	2.5	0.26	0	0.5	38669.3 ± 17928.7	6715.435 ± 3079.5
SHH-17	3.2	0.26	0	0.5	51446.4 ± 17240.2	7425.81 ± 2577.8
SHH-18	3.85	0.26	0	0.5	27671.3 ± 118.2	3907.52 ± 27.32
SHH-19	3.2	0.5	0	0.5	8247.18 ± 110.84	1175.81 ± 194.01
SHH-20	3.2	0.13	0	0.25	10659.11 ± 529.55	1727.18 ± 99.12
SHH-21	3.2	0.087	0	0.25	7419.45 ± 666.44	1162.74 ± 90.07
SHH-22	5	0.26	0	0.25	6668.32 ± 106.39	786.345 ± 66.16

Continued on next page

Table H.1 – continued from previous page

Sample #	**CNS (wt./v)**	**CB[7] (wt./v)**	**SPA (wt./v)**	**PAM (wt./v)**	**G'**	**G"**
SHH-23	3.2	0.26	0	0.25	22327.53 ± 6990.14	3022.52 ± 903.63
SHH-24	5	0.26	0	0.25	8290.03 ± 499.48	1031.96 ± 127.13
SHH-25	3.2	0.13	0	0.5	16948.10 ± 3243.58	2204.05 ± 569.22
SHH-26	3.2	0.086	0	0.5	16164.95 ± 1467.23	2230.47 ± 231.30
SHH-27	3.2	0.52	0	0.25	273.29 ± 131.53	45.13 ± 0.26

A p p e n d i x I

SHH DATA TABLE: PMPC

Table I.1: PMPC Samples.

Sample #	**CNS (wt./v)**	**CB[7] (wt./v)**	**SPA (wt./v)**	**PMPC (wt./v)**	**G'**	**G"**
	‰	‰	‰	‰	(Pa)	(Pa)
Control-14	2	0	0.14	0.25	839.2 ± 34.36	90.40 ± 10.18
Control-15	2.5	0	0	0.25	116.3 ± 101.7	17.3 ± 9.30
Control-16	3.2	0	0	0.25	268.0 ± 42.2	23.66 ± 3.18
Control-17	3.85	0	0	0.25	1085.9 ± 38.0	71.54 ± 2.84
Control-18	2.5	0	0	0.5	109.9 ± 40.1	20.28 ± 2.32
Control-19	3.2	0	0	0.5	489.0 ± 52.2	43.18 ± 3.74

Continued on next page

Table I.1 – continued from previous page

Sample #	**CNS (wt./v)**	**CB[7] (wt./v)**	**SPA (wt./v)**	**PMPC (wt./v)**	**G'**	**G"**
Control-20	3.85	0	0	0.5	1108.0 ± 20.0	86.61 ± 0.06
Control-21	2	0	0	0.25	69.67 ± 7.00	11.32 ± 0.261
Control-22	3.6	0	0	0.25	1467.27 ± 111.52	103.64 ± 9.55
Control-23	5	0	0	0.25	5225.63 ± 3362.67	331.07 ± 198.81
SHH-28	2	0.26	0.14	0.25	2792.37 ± 698.9	253.32 ± 57.53
SHH-29	3.2	0.26	0	0.25	1891.66 ± 68.09	276.35 ± 10.21
SHH-30	3.85	0.26	0	0.25	2784.67 ± 33.05	403.26 ± 16.14
SHH-31	2.5	0.26	0	0.25	1773.53 ± 1094.09	233.46 ± 113.20

Continued on next page

Table I.1 – continued from previous page

Sample #	**CNS (wt./v)**	**CB[7] (wt./v)**	**SPA (wt./v)**	**PMPC (wt./v)**	**G'**	**G"**
SHH-32	2.5	0.26	0	0.5	1132.29 ± 264.70	148.42 ± 37.31
SHH-33	3.2	0.26	0	0.5	2949.83 ± 231.43	349.28 ± 44.78
SHH-34	3.85	0.26	0	0.5	3782.2 ± 68.02	482.63 ± 7.83
SHH-35	3.2	0.5	0	0.5	4268.79 ± 2196.42	645 ± 307.90
SHH-36	4.47	0.26	0	0.25	24636.4 ± 3381.63	3690.53 ± 626.04
SHH-37	3.2	0.13	0	0.25	1385.75 ± 380.29	151.62 ± 49.07
SHH-38	3.2	0.087	0	0.25	1427.5 ± 202.03	127.09 ± 23.49
SHH-39	5	0.26	0	0.25	6965.76 ± 945.06	762.87 ± 100.23

Continued on next page

Table I.1 – continued from previous page

Sample #	**CNS (wt./v)**	**CB[7] (wt./v)**	**SPA (wt./v)**	**PMPC (wt./v)**	**G'**	**G"**
SHH-40	3.2	0.26	0	0.25	6075.43 ± 116.06	704.30 ± 33.89
SHH-41	5	0.26	0	0.25	6724.32 ± 1537.87	763.11 ± 194.92
SHH-42	2.5	0.26	0	0.25	2427.92 ± 440.47	278.12 ± 18.97
SHH-43	3.85	0.26	0	0.25	3831.93 ± 1206.01	480.31 ± 156.43
SHH-44	3.2	0.13	0	0.5	1007.35 ± 214.64	90.77 ± 25.50
SHH-45	3.2	0.086	0	0.5	538.64 ± 36.90	47.02 ± 5.02
SHH-46	3.2	0.52	0	0.25	7579.17 ± 501.45	788.16 ± 41.46
SHH-47	3.85	0.26	0	0.25	8331.31 ± 418.30	808.48 ± 83.45

Appendix J

SHH DATA TABLE: PEI & PMM+

Table J.1: PEI Samples.

Sample #	**CNS (wt./v)**	**CB[7] (wt./v)**	**SPA (wt./v)**	**PEI (wt./v)**	**G'**	**G"**
	%	%	%	%	(Pa)	(Pa)
Control-24	2	0	0.14	0.25	2547.76	347.47
SHH-48	3.2	0.26	0	0.25	2261.25 ± 781.56	314.79 ± 82.05

Table J.2: PMM+ Samples.

Sample #	**CNS (wt./v)**	**CB[7] (wt./v)**	**SPA (wt./v)**	**PMM+ (wt./v)**	**G'**	**G"**
	%	%	%	%	(Pa)	(Pa)
Control-25	2	0	0.14	0.25	878.03	70.39
SHH-49	3.2	0.26	0	0.25	23517.36 ± 1147.56	2866.31 ± 214.43

ADDITIONAL MATERIALS